

Deliverable Data			
Deliverable number	D4.2		
Deliverable name	Development and Characterization of a 200- mm diameter Pseudo-Active Mirror Disk Amplifier Module		
Work Package	WP 4		
Lead WP/deliverable beneficiary	Amplitude Laser	Amplitude	
Type and dissemination level	Report, public	Amplitude	
Deliverable status			
Submitting author	Florian Mollica		
Verified (WP leader)	Franck Falcoz / Pierre-Mary Paul		
Approved (Coordinator)	Vincent Bagnoud		
Due date of deliverable	30/06/2025		





## **Table of Contents**

Αl	bout	THRILL	1
E	xecu	tive summary	2
ΑI	bbre	viations	2
1.	I	Introduction and objectives	3
2.	(	Simulation and Optics procurement	4
	2.1	Illuminance simulations	4
	2.2	Simulation parameters	4
	2.3	Model comparison with the reference DAM Ø100mm	6
	2.4	Improved coupling in Ø-200mm PAMDAM	7
	2.5	Effect of distance between the flashlamps and the laser disks	7
	2.6	Cooling flow simulations	8
	2.7	Dichroic mirror characterization	10
3.	[	Design Principles	. 13
	3.1	Flashlamp Assembly	. 13
	3.2	Optical Assembly	. 15
	3.3	Optical test bench	. 16
4.	(	Optical Characterization	. 18
	4.1	Transmission	. 18
	4.2	Tested Fluid	. 18
	4.3	LIDT tests at 1053nm	. 19
	4.4	Flashlamp Irradiation	. 19



	4.5	Small signal gain	22
		Fluorescence	
		Birefringence	
		Wavefront Distortion	
	4.9	Pointing Stability	45
5.	(	Conclusion	47
	5.1	Project continuity	48
6.	I	Bibliography	49

#### **Disclaimer**

This document is part of the deliverables from the project THRILL, which has received funding from the European Union. Views and opinions expressed are however those of the author(s) only and do not necessarily reflect those of the European Union or the European Commission. Neither the European Union nor the granting authority can be held responsible for them.



### **About THRILL**

The THRILL project deals with providing new schemes and devices for pushing forward the limits of research infrastructures (RI) of European relevance and ESFRI landmarks. To do so, the project partners have identified several technical bottlenecks in high-energy high-repetition-rate laser technology that prevent it from reaching the technical readiness level required to technically specify and build the needed devices, and guaranteeing sustainable and reliable operation of such laser beamlines at the partnering RIs. Advancing the technical readiness of these topics is strategically aligned with the long-term plans and evolution of the ESFRI landmarks FAIR, ELI (-BL) and EuXFEL, and RI APOLLON, bringing them to the next level of development and strengthening their leading position.

The project is focused and deliberately restricted to three enabling technologies, which require the most urgent efforts and timely attention by the community: high-energy high-repetition-rate amplification, high-energy beam transport and optical coating resilience for large optics. To reach our goals, the major activity within THRILL will be organized around producing several prototypes demonstrating a high level of technical readiness. Our proposal is addressing not yet explored technical bottlenecks - such as transport over long distances of large-aperture laser beams via relay imaging using all-reflective optics - and aims at proposing concrete steps to increase the performances and effectiveness of the industrial community through the co-development of advanced technologies up to prototyping in operational environments.

The project is not only pushing technology, it is also offering an outstanding opportunity to train a qualified work force for RIs and industry. With this in mind, the structure of THRILL promotes synergetic work, fast transfer to industry and integrated research activities at the European level. Access to the RIs will be granted as in-kind contribution.



# **Executive summary**

In the past 6 years, Amplitude has developed a 100-mm Pseudo Active Mirror Disk Amplifier Module (PAMDAM) with neodymium-doped phosphate glass and Nd: YAG laser material. The attainable level of energy is > 200 J at 0.1 Hz and 75 J at 10 Hz, respectively. In the framework of THRILL, we aim to upsize the module to 200 mm Nd: glass disks.

## **Abbreviations**

Abbreviation	<b>Definition</b>
PAMDAM	Pseudo-Active Mirror Disk Amplifier Module
ASE	Amplified Spontaneous Emission
g0L	Small-signal gain
SR	Strehl ratio
Nd:Glass	Neodymium-doped phosphate laser glass
λΡV	Amplitude of wavefront deformation PV (Peak to Valley) in λ (1053nm)
AOI	Angle of Incidence (measured from the normal axis)



# 1. Introduction and objectives

Over the past decade, new systems have sought to fill the 100J-1kJ range with higher repetition rates compatible with industrial applications, DIPOLE (Mason, 2017), L4-ATON (Condamine, 2022)

The announcement by NIF of promising results in inertial confinement fusion has revived interest in kJ sources with higher repetition rates. (Batani D, 2023)

In the past 6 years, Amplitude has developed a 100-mm liquid cooled Pseudo Active Mirror Disk Amplifier Module (PAMDAM), with neodymium-doped phosphate glass (Hernandez, et al., 2024) and Nd:YAG laser material (Roland S. Nagymihály & Kalashnikov, 2023). The attainable level of energy is > 200 J at 0.1 Hz and 75 J at 10 Hz, respectively. Different technologies exist for thermal management of the slabs subject to high repetition flash discharges: cryogenic cooling (Mason, 2017), high-speed gas-flow (Andy Bayramian & Barty, 2008) and liquid cooling (Pierre-Marie Dalbies, Nov 2023) (Kelly, 1981), but liquid cooling present the most efficient way to extract thermal load due to higher density than gas. The idea of improving the lamp coupling and the cooling efficiency with an active mirror was studied for a long time (D. Brown, 1981), but Amplitude innovated with a Pseudo-active Mirror concept that split the active laser material from the mirror.

In the framework of THRILL, we aim to upsize the module to 200 mm Nd:glass disks. It requires mechanical, thermo-mechanical, and fluidic simulations followed by the optical and mechanical design of the PAMDAM prototype. A major challenge lies in the implementation of components such as unique and complex dichroic mirrors and large diameter Nd: glass disks. Such disks with a high emission cross-section which are hard to obtain (2 suppliers only) and the related lead time of these critical components. A specific flow shaping design homogenizes the coolant flow to maximize the wavefront quality.

Taking advantage on the knowledge acquired on the 100-mm model, Amplitude aims to increase the coupling between the flashlamp and the disks. The laser energy output is limited in the 100-mm model by a low transmission (<90%), and the attempt of AR coating on the disks failed because of the degradation caused by cooling water on Nd-doped phosphate glass. One of the innovations of this program is to evaluate novel fluids never used in laser environments that could be of great interest both for amplifiers transmission and for limitation of parasitic oscillations.

Parasitic oscillations in laser material rise proportionally to the transverse dimension of the disks, and upscaling from 100 mm to 200 mm requires an improved management of parasitic oscillation.



# 2. Simulation and Optics procurement

#### 2.1 Illuminance simulations

Illuminance simulations are performed on COMSOL Ray Tracing, the goal is twofold: first, being able to derive the geometric coupling between the flashlamp illumination and the laser disk absorbance. Second is to find a Ø-200mm design yielding more gain than the previous Ø-100mm DAM version.

Such simulation is challenging.

- 1. Flash lamp emission is broadband with a current-dependent spectrum.
- 2. Lamp cross-absorption is spectrum and current-dependent.
- 3. Lamp re-emission is not well understood.
- 4. Multiple ray divisions are computationally challenging.

To overcome those challenges, we compared the design of THRILL PAMDAM with the existing design of PremiumLite Ø100mm DAM in a simplified static model:

- The figure of merit is the laser gain, which is proportional to absorbed energy per medium gain surface. [J/cm2]
- Single wavelength simulation for a strong absorbing line of laser disk.[alpha@1%wt @525nm = 1cm<sup>-1</sup>]
- Flash lamp opacity derived from a '94 Livermore publication in the most absorbent configuration (peak current in the flashlamp) [alpha Xe @3kA@525nm =1,28cm<sup>-1</sup>]
- Flash lamp emission is Lambertian on Xenon surface with random direction.

## 2.2 Simulation parameters

#### 2.2.1 Energy conservation

On each interface the rays are split into a refracted and transmitted ray, while a criterion either on the number of sub-ray or the power of each ray discard extra rays to not overload the simulation. In this condition, it is important to check energy conservation. Using an upper limit of 1M secondary rays + discarding every ray < 1:100 of the main ray, we could keep an energy conservation of 95%.

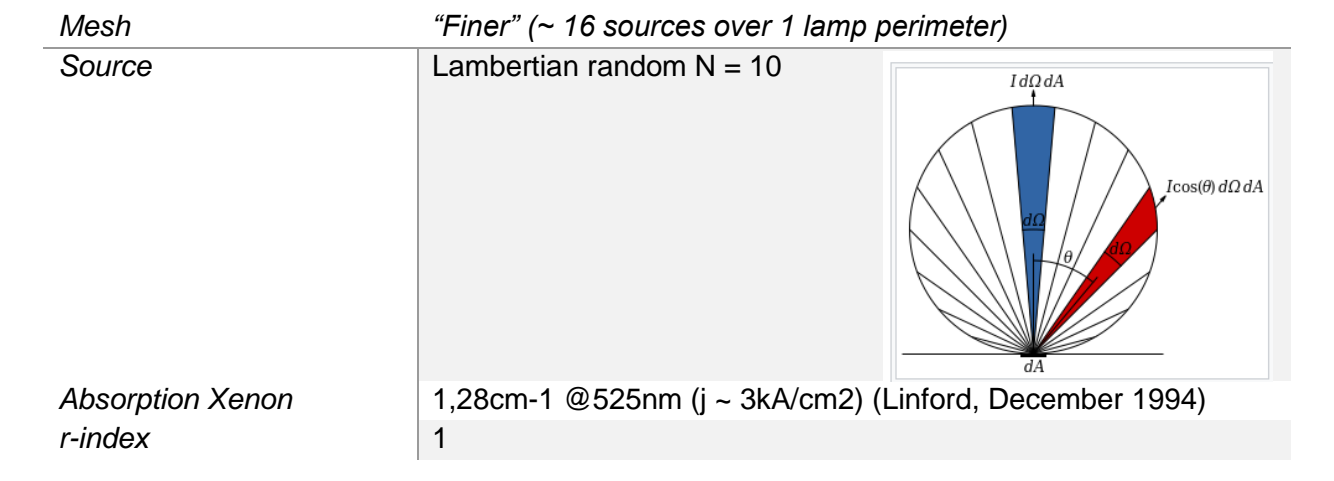
#### 2.2.2 Flashlamps

Each lamp is modelized by ~1300 sources firing 10 rays each. Two flashlamp models have been tested in reduced configurations:



- Realistic: Each lamp is made of a cylinder of Xenon surrounded by a shell of 1mm Quartz
- Simplified: Each lamp is made only of a cylinder of Xenon

By reducing the interface number, the simplified model decreases the computational power needed. Each model yields the same illumination, and the same cross lamp absorption. It should be noted that the ray tracing simulation **is static** while the plasma absorption is proportional to the current (it changes during the discharge) and the wavelength. Here the Xenon opacity is set to its maximum value. (Linford, December 1994).



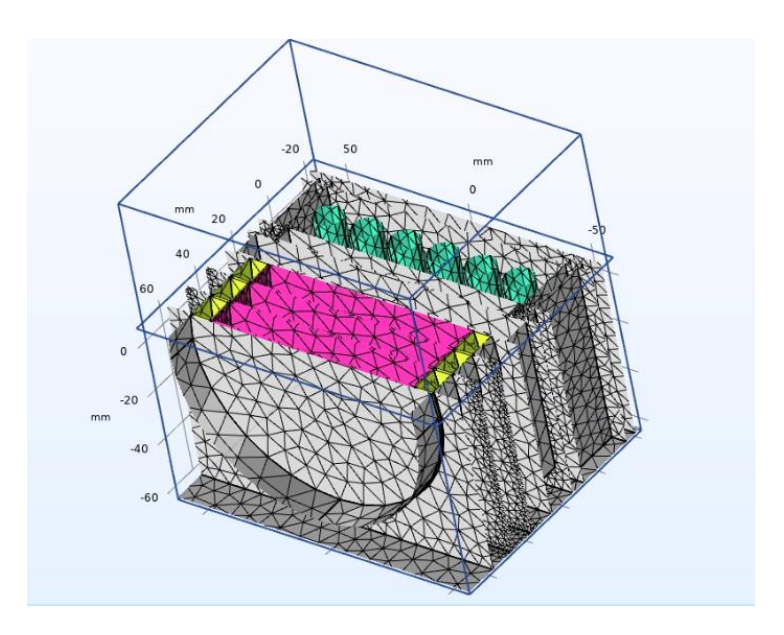


Figure 1: Mesh example for the PAMDAM 100-mm model. In pink the laser disks, in yellow the cladding, in green the flashlamps.



#### 2.2.3 Laser Disks

Mesh	~50 mesh element over the diameter ~20 mesh element in disk thickness
Absorption Laser material	Depending on the incoming spectrum: two values evaluated: Set to α=1cm-1 for 1% wt. Nd doping (523nm) Set to α=0.1cm-1 for 1% wt. Nd doping (686 nm)
Dimension	Ø170mm
r-index	1.5

#### 2.2.4 Reflective ceramics

The ceramic behind the flashlamp is modeled by a near perfect diffusive reflector, according to the provider spec sheet.

Reflectivity across spectrum	98%
Reflectivity mode	Lambertian diffusion

# 2.3 Model comparison with the reference DAM Ø100mm

The small signal gain of the reference DAM Ø100mm is measured at a maximum of 0.24 with 6 flashlamps of arc length 100mm. For the Ø200mm version we used lamps of arc length 200mm, with similar spectral emission.

A small signal gain of 0.24 corresponds to an absorbed energy of 65J into the disks, achieved by a geometrical coupling between the flashlamp light and the disks of 45% according to our simple 1D spectral model.

COMSOL results shows a geometrical coupling efficiency for 525nm light ( $\alpha$  = 1cm-1 in 1% doping laser medium) in the Ø100m DAM shows a coupling of 41%, while 40% of this wavelength is self-absorbed by the lamp. The rest is lost through the outer dichroic mirror, the inner reflections, or the numerical losses of discarded secondary rays (up to 10% in this simulation).

For 686nm light ( $\alpha$  = 0.1cm-1 in 1% doping laser medium) the coupling drops to 30%. Weakly absorbed wavelength endures extra reflection into the disk cavity, it means that more reflections losses are expected, explaining this lower value.

It is important to recall that this simulation does not account for the spectral distribution of flashlamps, nor the spectral absorption of laser disks and the electrical losses between the



capacitor bank and the lamp plasma emission. It gives an idea of the geometrical coupling for a given absorption alpha. It is reassuring that the value of 40-45% is found both in this ray tracing simulation and our measurement of the PAMDAM 100mm.

## 2.4 Improved coupling in Ø-200mm PAMDAM

We computed here the geometrical coupling at 525nm ( $\alpha$  = 1 cm-1 for Nd-doping of 1% wt.) for the DAM  $\emptyset$ 200mm.

Disks in the PADMAM 200mm are 4 time larger than disks in the PAMDAM 100mm, with 4 time the lamps output, the simulation should yield roughly the same absorbed energy in the disks for an homothetic configuration.

The simulation confirms that the geometrical coupling is similar in the 100mm reference case vs the 200mm version, for an homothetic configuration, around ~42%.

We simulated an upgraded version where coupling is improved and stored energy in the disks rise from 240J to 300J

The coupling is also computed with another wavelength (686nm) where the disk absorbance for 1%wt. Nd-doping is  $\alpha = 0.1$  cm-1 (10% of 525nm). While the geometric coupling is ~30% worse, it varies in the same proportion from the homothetic to the improved configuration.

Such results if demonstrated are well above similar 1shot/min, actively cooled Nd:Glass amplifiers: 0.2 in active mirror (Kelly, 1981), 0.14 in liquid cooled Brewster slabs amplifier (Pierre-Marie Dalbies, Nov 2023) or 0.2 in Apollon CNE (Garrec, 2022)

DAM Model	DAM Ø100mm	DAM Ø200mm improved version	DAM Ø200mm homothetic version
Voltage	2400V	2400V	2400V
Surface laser disk [cm2]	56,7	227	227
g0L	0,24*	0,302*	0,243*
Stored energy per DAM	65	301	242

<sup>\*</sup> The small signal gain 0.24 for the reference DAM Ø100mm is measured in configuration with optimal disk coating. For the Ø200mm DAM, the gain is derived from the computed absorbed energy.

# 2.5 Effect of distance between the flashlamps and the



#### laser disks

Increasing the distance between flashlamps and the medium decreases the gain by 0,4% per mm. This stays true as well for wavelength with low absorption (0,1cm-1) in the laser medium.

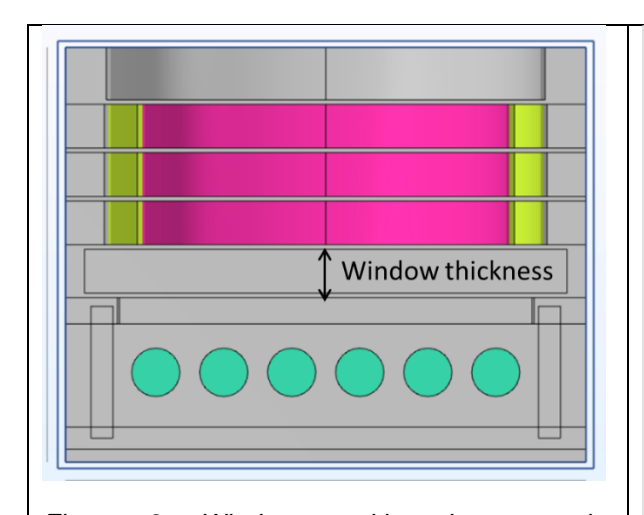
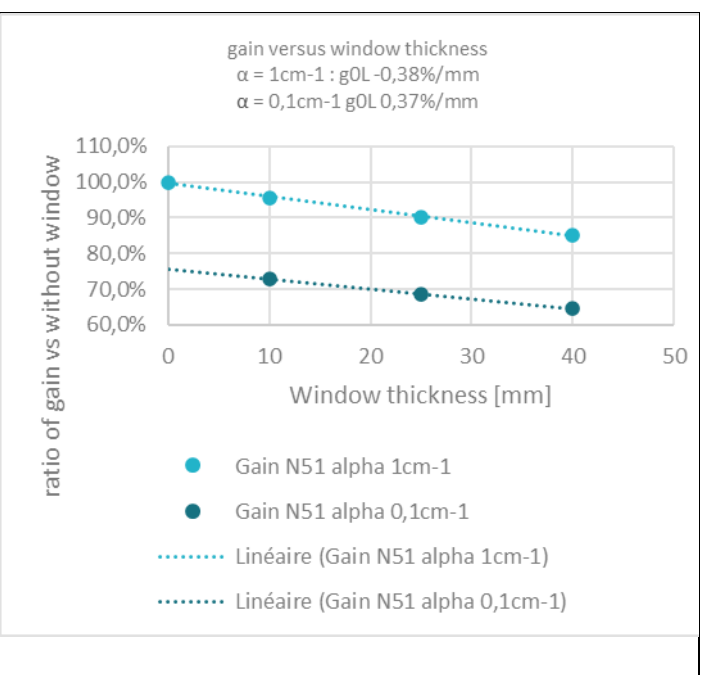


Figure 2: Window position between the flashlamp assembly and the disk assembly. The incoming laser light comes from the top, reflects on the internal dichroic mirror, and exits back via the entry dichroic mirror



## 2.6 Cooling flow simulations

Cooling of the disks is performed by a laminar flow on the large disk surface. Specific care in the mechanical design has been taken to ensure a regular flow, without steps or dents that could perturbate the flow.

The disks absorb around 6% (empirical value) of the flashlamp electrical energy (minus the part self-absorb by the lamps) as heat. The cooling fluid extracts this heat by flowing on the large disks face through thin channel. At 0.05Hz 150W need to dissipate from the disk's surfaces. A limited temperature increase of the cooling fluid of 0.4°C between inlet and exit is expected, limiting the risks of refraction fringes. These fringes can emerge because of slight variation of velocity over a hot disk, leading to variation in temperature. In water a local variation of  $\Delta T = 0.1$ °C can lead to an optical path difference of  $\lambda/4$  over few mm, enough to damage the wavefront locally.



To dissipate in THRILI disks 0.05Hz	L 0,15 kW
Fluid	CHCl₃
Inlet temp.	20 °C
Outlet temp.	20,4 °C
Flow	16 l/min
Max pressure drop.	1,3 Bars

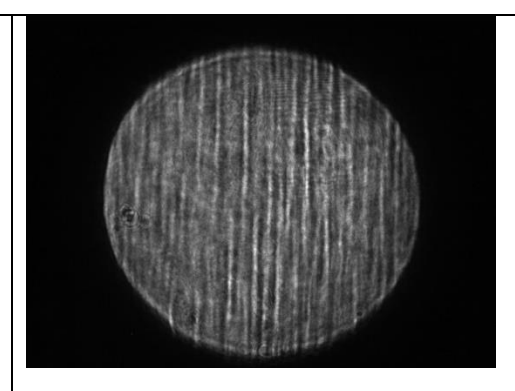


Figure 3: Example of flow fringes due to inhomogeneity of temperature and flow velocity in the D100mm YAG PAMDAM (500W to dissipate)

A **specific flow smoothing system** homogenizes the fluid velocity transversally. Simulations show that velocity dispersion could be as low as 0.16% Peak to Peak.

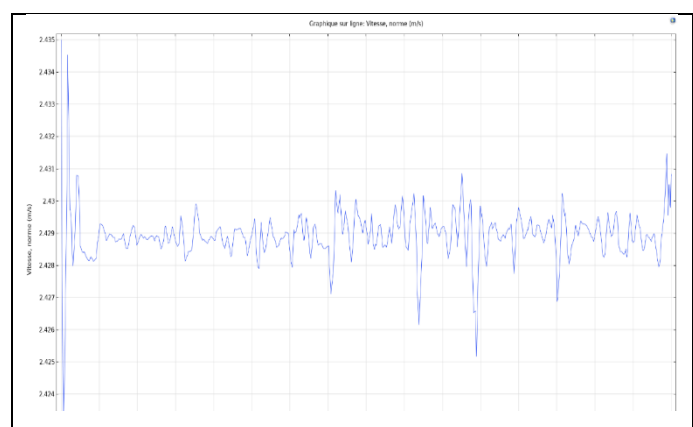


Figure 4: Transverse Lineout of fluid velocity in the center of the laser disks cooling channel. (Simulation) Inhomogeneity are only 0.16% PP

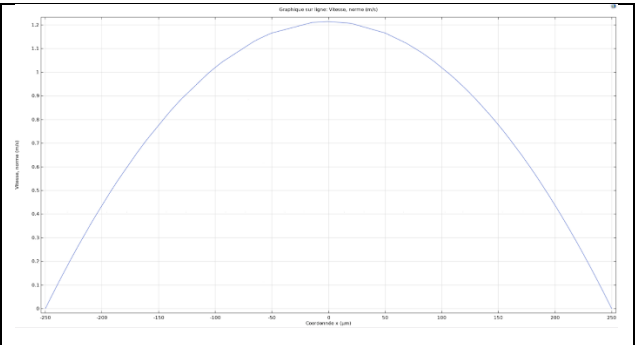


Figure 5 :fluid velocity distribution in a cooling channel along the 500µm of channel thickness for 4l/min/channel.



#### 2.7 Dichroic mirror characterization

The internal dichroic mirror is critical in the PAMDAM design. Its aim is to transmit the incoming pump light from the flashlamps with minimal losses while reflecting the 1053nm laser. Procurement of large dichroic mirror was a risk identified at the start of the project. Sample characterization in LIDT and spectral transmission have been performed before large pieces procurement and are described in the next section.

#### 2.7.1 LIDT Measurement



Figure 6: LIDT set-up for external dichroic mirror (AR1053 + HR VIS)

A Titan laser delivers a maximum of 5.6 J at 5 Hz over Ø 20mm. A half waveplate and polarizer adjusts the beam energy.

A lens focused the beam on the sample with a 3° AOI. The 7.5 mm@1/e2 diameters allows a maximum average fluence of ~14 J/cm² in Polarization P. Spatial inhomogeneities in the beam make the maximum fluence (peak) higher (x1.54 the average fluence of the plateau).

The temporal shape is gaussian with 10.8 ns at FWHM. For each provider and both dichroic models, two to three samples were tested on different site in 1000-on-1 configurations. If the test was successful, a longer test of 9000 shots were performed.



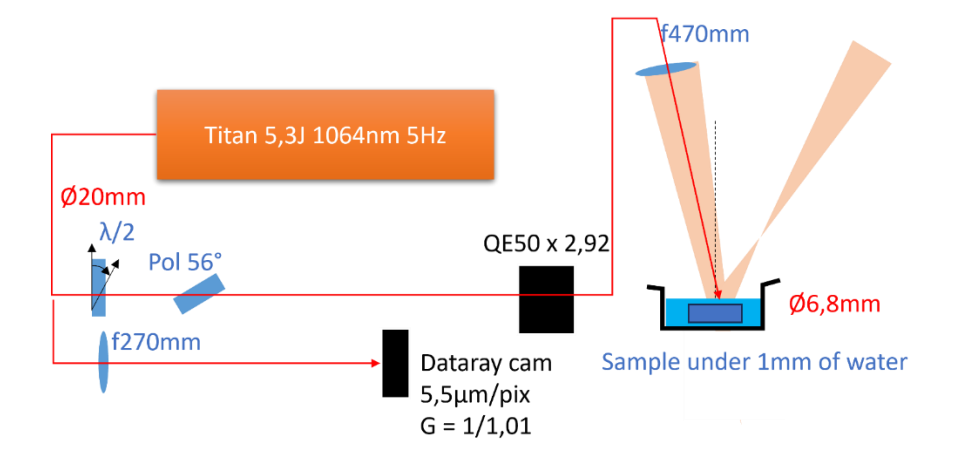


Figure 7: LIDT set-up for internal dichroic mirror (HR1053 + AR VIS)

Table 1: LIDT @10ns @1053nm for the sample tested for the two providers and both model of dichroic. The LIDT is given as the mean fluence over a diameter of 7.5mm. The value in () is the maximal intensity hot spot observed on the beam profile.

	Provider #1	Provider #2
Internal dichroic mirror (HR 1053nm + AR VIS)	3.5 J/cm2 (5.6 J/cm2)	8.9 J/cm2 (14 J/cm2)
External dichroic mirror (HR VIS + AR 1053nm)	14.7 J/cm2 (19.2 J/cm2)	6J /cm2 (8 J/cm2)

#### 2.7.2 Internal dichroic transmission

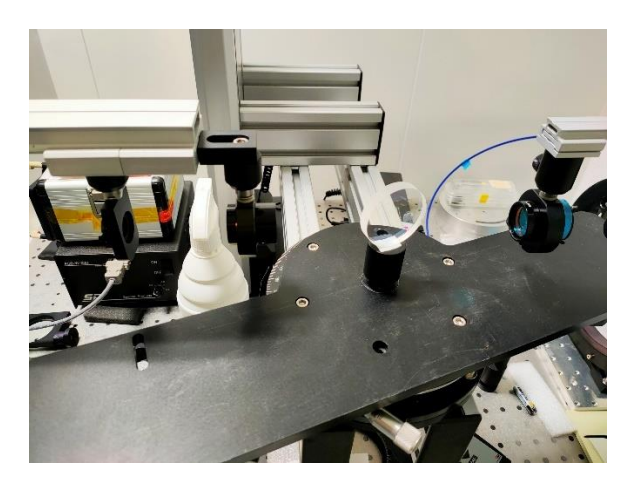


Figure 8: Optical bench for angular transmission measurements with a white light.

Our optical bench allows angular- and spectrally resolved transmission measurements for wavelength from 660 to 950nm. Transmission of the non-coated face must be removed. In this range the transmission meets the specifications. Transmission at large angles is measured as the flashlamp light can intersect the coating all angles. Measurement is made with a mixed polarization from the white light source. The coating is designed to be in water.

Table 2: Mean Transmission in Air for a given angle of incidence between 660 and 946nm for internal



#### dichroic mirror samples. Avg Polarization

Angle of Incidence (in Air)	Provider #1	Provider #2
0°	93.9%	90.4%
60°	70.9%	71.5%

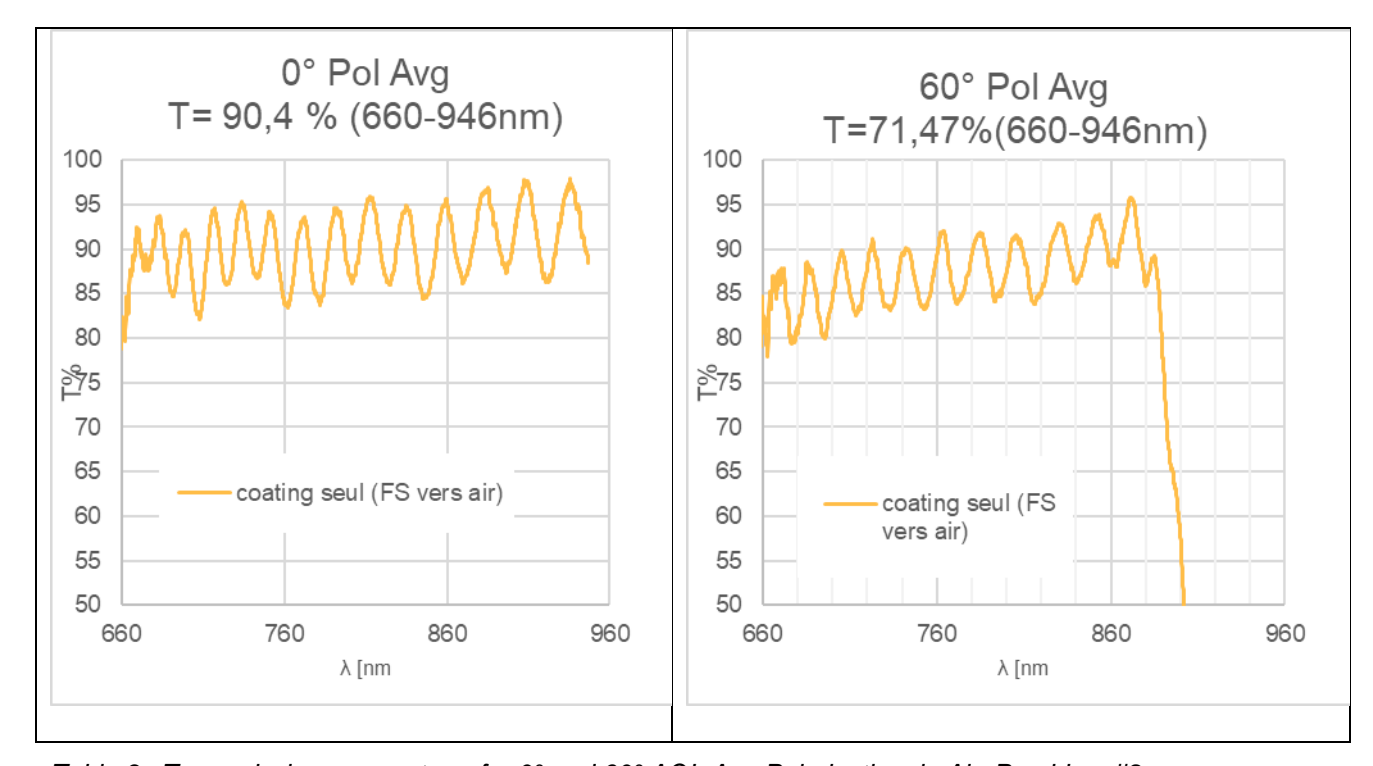


Table 3: Transmission vs spectrum for 0° and 60° AOI, Avg Polarization, in Air. Providers #2



# 3. Design Principles

The following table shows the expected energy at 1053nm a full laser system made of 6 PAMDAM could deliver at 1shot/min, depending on the amplifier properties. Injection is 25J in 10ns FWHM. It shows the critical importance of gain and transmission on the final characteristic of a full system, and the design goal.

goL /T%	0,24	0,28	0,3	
93%	608 J	823 J	924 J	
97%	794 J	1037 J	1151 J	

Figure 9: Expected energy at the output of a laser system of 6 PAMDAM with the transmission and gain per head (gain given in simple pass)

## 3.1 Flashlamp Assembly

Flashlamp Assembly is made of 3 layers with different purposes :

- From the outside, an insulation, heat-resistant plastic protects the user and the optical assembly from high currents and voltages.
- Inside, a conductive assembly surrounds the flashlamps and enables triggering (breakdown of the lamp impedance). The conductive shell is linked to the trigger circuit through the insulating plastic.
- Finally, a broadband, high-angle reflective material surrounds the flashlamps and recycles the flashlamp light towards the laser disks.

Lamps are filled with Xenon. They are made of cerium-doped quartz to filter out the UV light from the hot plasma. Arc discharge is 200mm long.

Flashlamp assembly can be filled with a fluid independent from the Optical Assembly because it is sealed with a Fused Silicate window. Mostly 99% deuterated water has been used in this experimental campaign.

An electrical test campaign of 3 weeks enabled 10k shots at 2300V without lamp break or misfire. The following month confirmed the reliability of the discharge. Each lamp is monitored independently thanks to the pseudo-simmer embedded function. The simmer current keeping the lamp impedance low and maintaining the plasma inside the lamp is monitored. If it drops before the



shot, action like shot cancellation can be performed, and the faulty lamps are located.

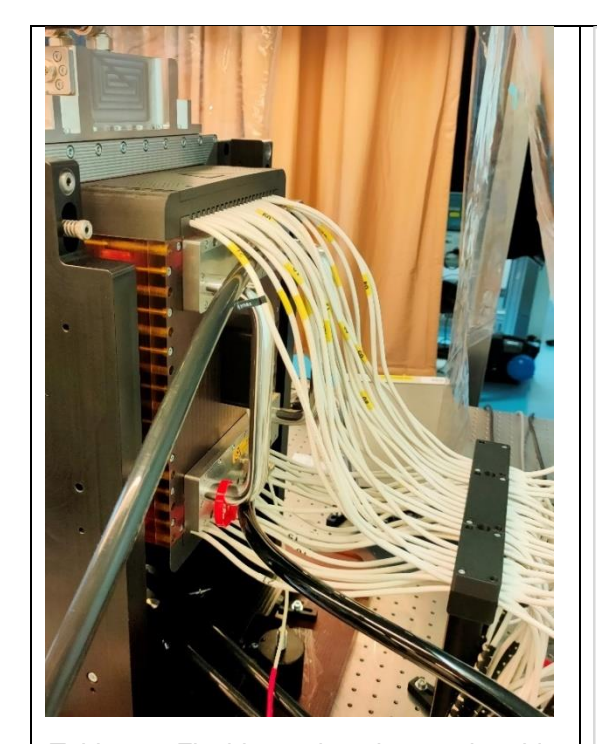


Table 4: Flashlamp housing and cable from the flashlamps.

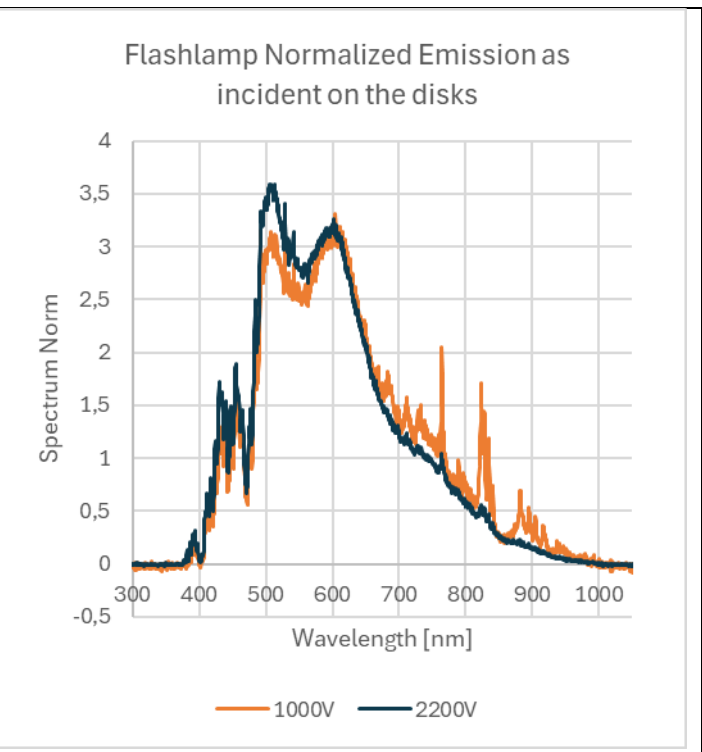
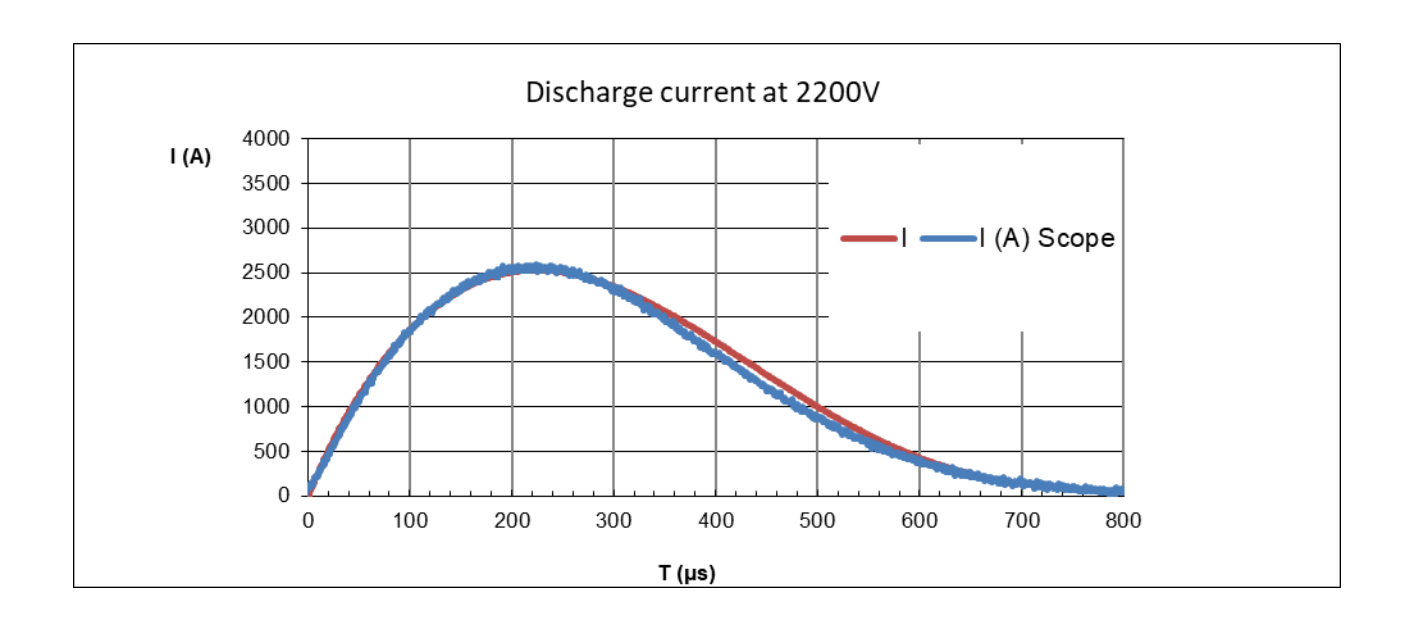


Figure 10: Xenon lamp spectrum.





# 3.2 Optical Assembly

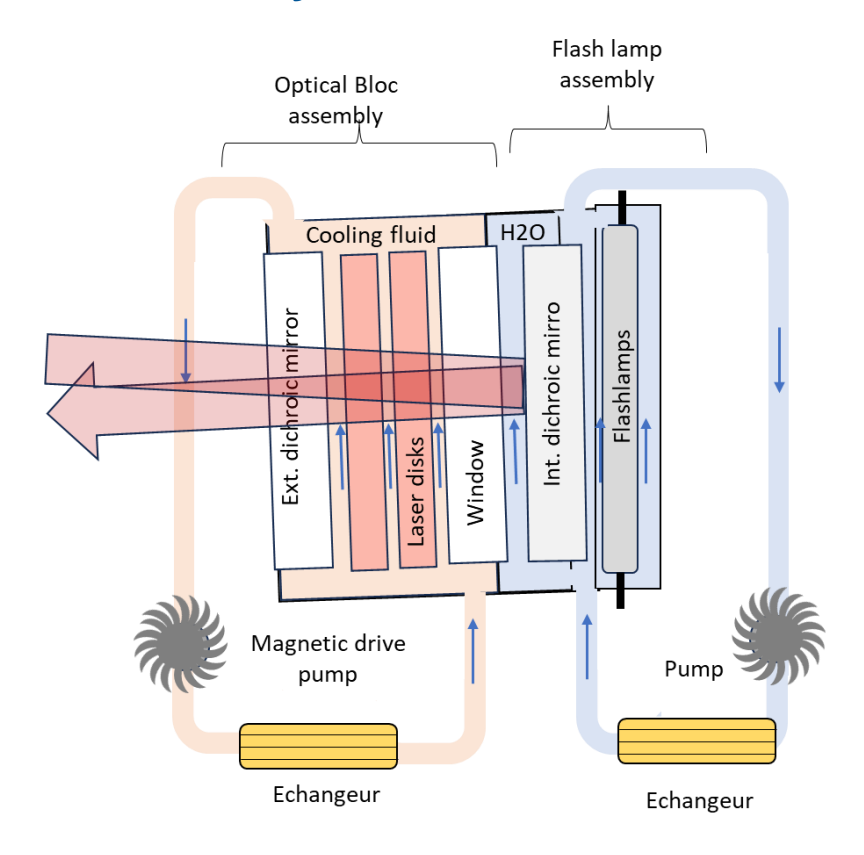


Figure 11: Schematic of the 200mm PAMDAM with two cooling fluids circuits, one for the flash lamps and one for the optical assembly, separated by a window. Dichroic mirrors enable the transmission and reflection of the incoming IR beam and the transmission of the lamps white light.

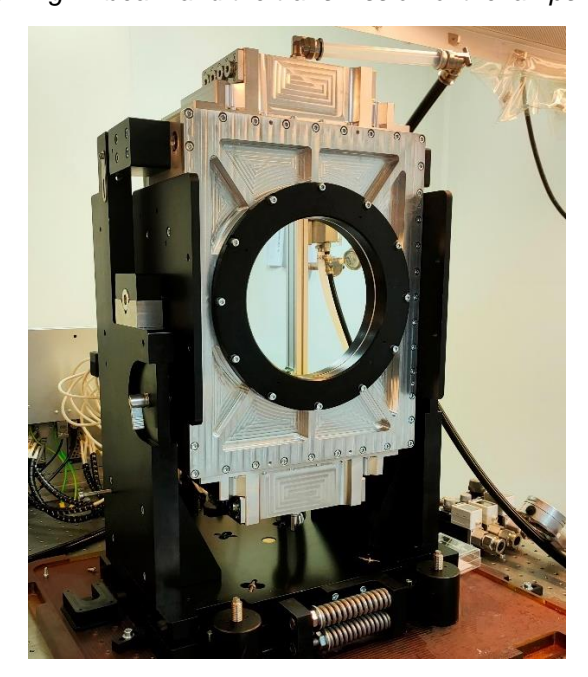


Figure 12: Front view of the external dichroic mirror and the PAMDAM inside its gimbal mount



## 3.3 Optical test bench

The optical test bench is designed to test the following parameters:

- Gain and Gain distribution
- Wavefront deformation
- Birefringence
- Near Field and Far field profile
- Pointing Stability

The first campaign from October 2024 to April 2025 use a Multi-order 5 Hz 1053 nm Q-switch laser (MiniLite) as a source, delivering ~15 mJ in gaussian pulses of 20 ns FWHM. To improve the beam spatial quality and stability, an improved source was developed.

The MiniLite cavity is "pinholed" to deliver 3 mJ in a TEM00 mode. Then it is amplified in 2-pass D7mm YLF Rod Amplifier delivering up to 90mJ of energy in 20ns FMHM. The beam is adjusted in shape to be roughly top hat over a diameter of 160 mm. This extra energy enables the increase of the signal to noise ratio in gain measurement, as the flash lamp discharge can generate up to 2-3mJ of noise. The last telescope toward the PAMDAM is either made from f+100mm/f2000mm lenses for imaging application at low energy -3mJ), or f-100mm/f2000mm lenses for high energy (90mJ) gain measurement.

For Near Field, Far Field and Wavefront measurement, the beam energy is reduced to 3mJ and a 2-step demagnifying telescope is used. The first telescope decreases the beam size by x1/20 while a second telescope adjusts the size for the various diagnostics while adding filtering (RG850 glass, Interferometric filter and polarizing cube). The image plane of the PAMDAM is relay imaged on the Near Field camera (Beamage-3.0, 2048 x 1088 pixels, 5.5µm x 5.5µm, 11.3 \* 6.0 mm) and Wavefront sensor (SID4 HR from Phasics, 9.98 x 8.64 mm², 416 x 360 phase pixels)



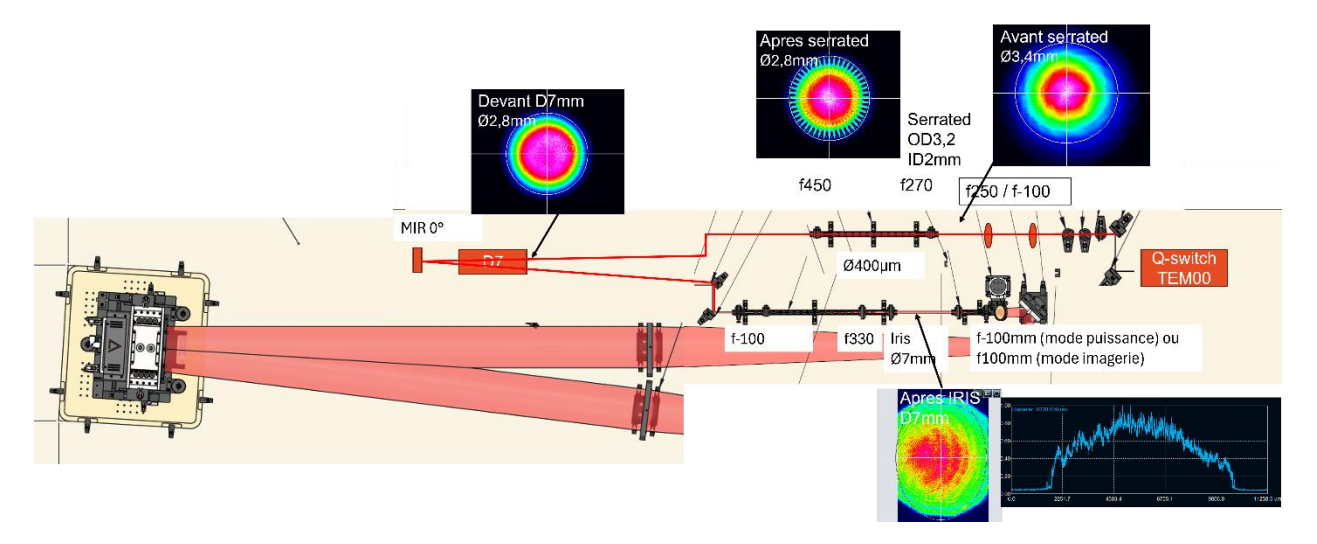


Figure 13: Source delivery layout for the TEM00 MiniLite and image relay to the PAMDAM.

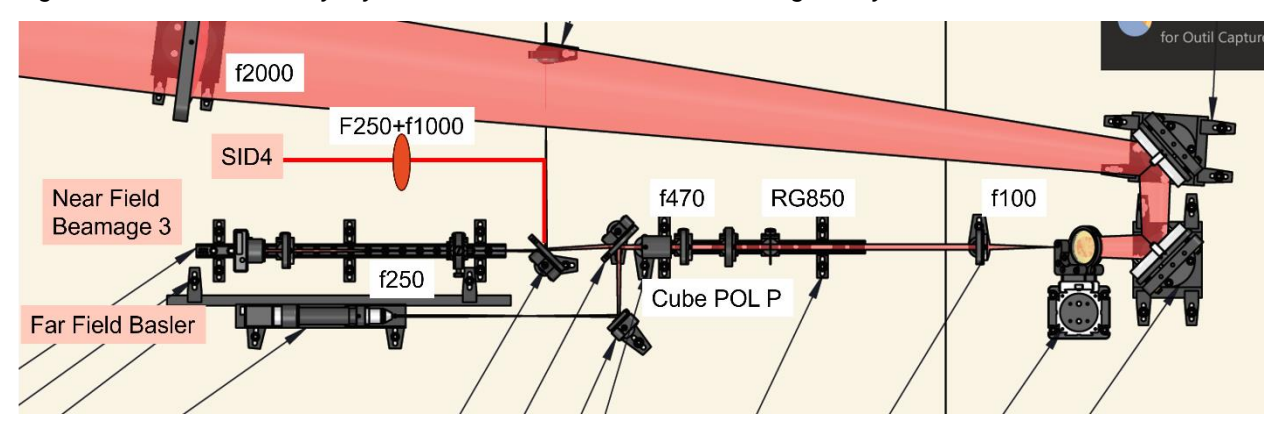


Figure 14: Diagnostics layout and image relay from the PAMDAM.

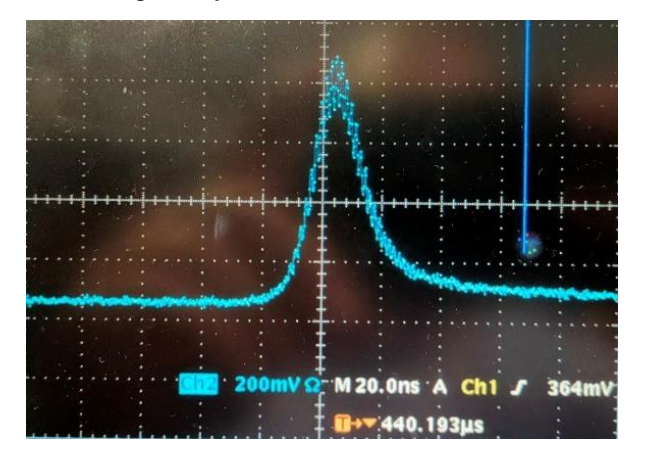


Figure 15: Beam temporal profile after amplification: D7: 1400V; DAM 2200V; FWHM = 20ns



# 4. Optical Characterization

#### 4.1 Transmission

PAMDAM Transmission and gain properties are very dependent on the chosen cooling fluid. Here are the technical constraints the fluid must obey:

- Transparent at 1053nm
- Transparent between 400 and 850nm (flash lamp spectrum)
- Resistant to intense flashlight and LIDT above 8J/cm2
- Inert with laser materials

Other properties are useful.

- High refractive index at 1053nm (close to the laser material index ~1.5) )
- High thermal capacity

Previous Ø100mm PAMDAM version used water as a cooling fluid, for its high thermal capacity, transparency in VIS light and relatively high index. Two issues prompted a search for a new fluid:

- Water dissolve laser disk at a rate of 100nm/day at 50°C, making surfaces rough and diffusive over time and removing coatings.
- Water refractive index at 1053nm (1.326) is far from laser disks r-index (1.5), resulting in transmission loss at each interface of ~0.4%. The high number of interfaces crossed by the laser in a PAMDAM results in a low transmission of 90-93%, limiting the total energy one can extract from a PAMDAM.

## 4.2 Tested Fluid

Here is the fluid list tested during in the PAMDAM THRILL Prototype

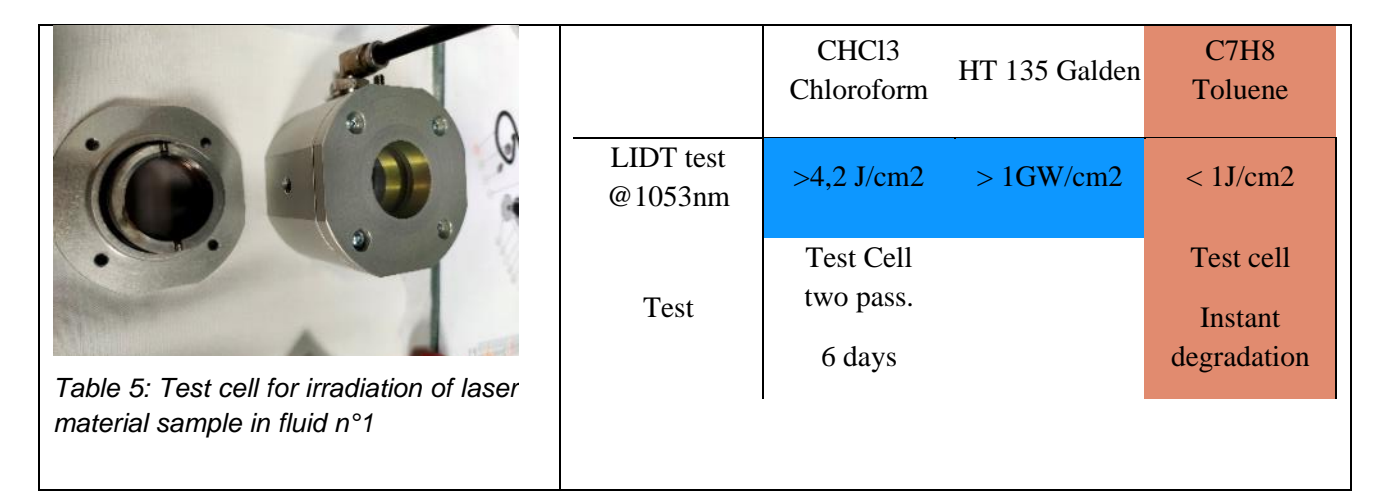
	D2O Heavy water	CHCI3 Chloroform, Trichloromethane	HT 135 Galden	C7H8 Toluene
Dynamic Viscosity @ 20°C, mPa.s (cP)	1,2460	0,5630	1,72	0,5600
Density,	1,105	1,564	1,72	0,8623
Heat capacity Cp, J/(g.°C)	4,242	0,9571	0,9614	1,707
Solubility in		benzene		acetone, diethyl oxide, chloroform,



				ethanol
Optical index @ 1053nm	1,32264	1,4354	1,28	1,4814
lineic abs, cm-1 @ 1053nm	0,022	0,00639	<0,001	0,0184
First ionization energy, eV	~9,5	11,42	>11	8,83
Risks/Drawbacks	Dissolve Laser glasses. Low refractive index	Partially Toxic Low heat capacity	Low heat capacity Low refractive index	Flammable, flash point @ 4°C, explosive @ 1,1-7,1%, autoignition @ 480°C
Quality	Best heat capacity Good transmission	High refractive index Great transmission	Inert Great transmission	Great transmission High refractive index

#### 4.3 LIDT tests at 1053nm

LIDT for Toluene is performed in a test tube, it is degraded at a fluence < 1J/cm2. LIDT for Chloroform is tested 6 days in double pass cell @ 4,2J/cm2 @11ns without degradation. Galden HT 135 LIDT was qualified in other experiments at intensity >1GW/cm2.



# 4.4 Flashlamp Irradiation

Chloroform and Galden HT 135 are tested in the PAMDAM without circulation and the PAMDAM Voltage transmission is monitored over 10 days.



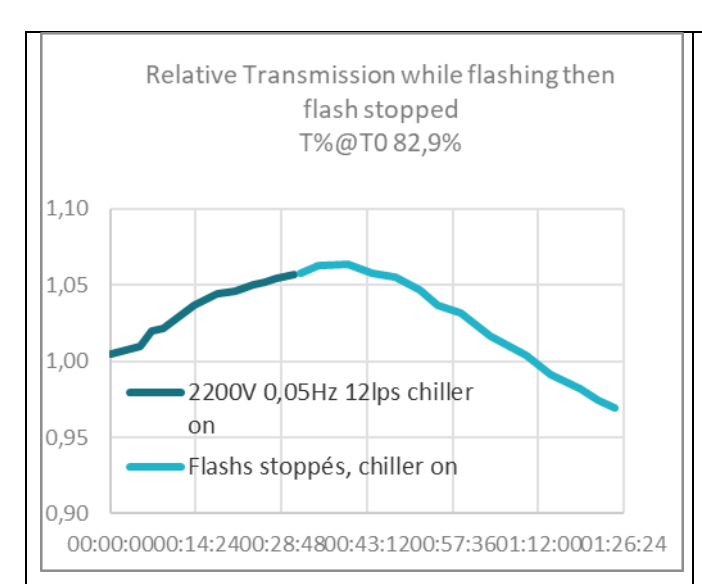


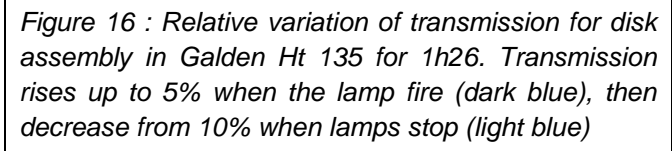
	D2O	CHCl3 Chloroform,	HT 135 Galden
LIDT test @1053nm		>4,2 J/cm2	> 1GW/cm2
Resistance to flashlamp light	ok	Black after 10s of shots	Slow degradation

Table 6: Degradation from fluid n°1 on the laser disks

After 1 day of irradiation with flashlamps at 2200V, chloroform experiences total degradation and black waste appears. The transmission is altered. (see figures)

For Galden HT 135 the transmission at 1053nm is stable for 3 weeks, but then it becomes highly unstable, with variation in few hours, even with just the chiller ON, without flashlamp.





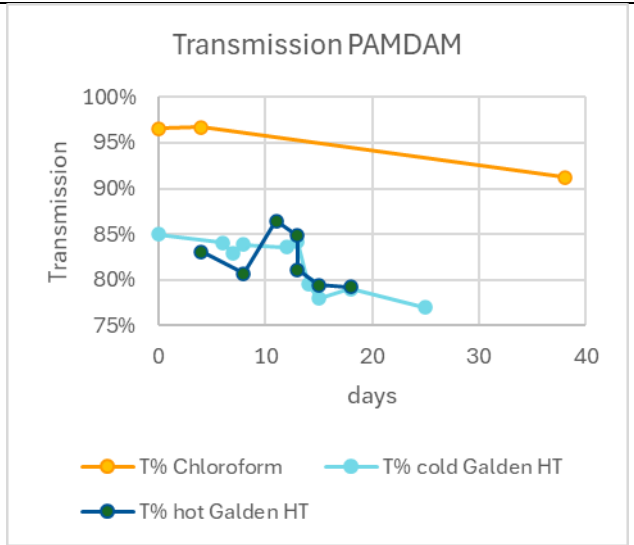


Figure 17: PAMDAM transmission evolution for several days. Static chloroform (orange) and Galden HT 135 (dark blue: hot, light blue: cold))

Tests of transmission are performed in a 10mm square quartz test cell. These tests show that just after sampling the fluid from the cooling circuit, the transmission is down to 86% (to compare with



98% with clean fluid see Fig below) and rises slowly while at rest the next 1h to settle at 94%. While no cause can be identified, the presence of a pollution mixed with the fluid is probable and get mixed when the chiller is on. Another supposition is the degradation of the Galden in subcomponents, recombining slowly over time.

	H2O	CHCI3 Chloroform	HT 135 Galden	C7H8 Toluene
LIDT test @1053nm		>4,2 J/cm2	> 1GW/cm2	< 1J/cm2
Theorical Transmission*	92,2%	97,2%	89%	
DAM Transmission (A/R)	87,2 %	96,5%	84%	
Degradation vs Time	none	Black after 10s of shots	Slow degradation	

Back and forth transmission is measured for the PAMDAM with different fluids, the first transmission - measured in chloroform - is very consistent with the Snell-Descartes laws. Transmission in Galden HT is expected to be lower than with water, as the refractive index of 1.28 is further from the laser disk's one. But transmission in Water and Galden are both lower than expected from theoretical value, either because the disks surface becomes rough and diffusive or the disk absorbs more than expected at 1053nm.

# 4.4.1 Sampling of Galden HT135 and transmission testing in square quartz test tube

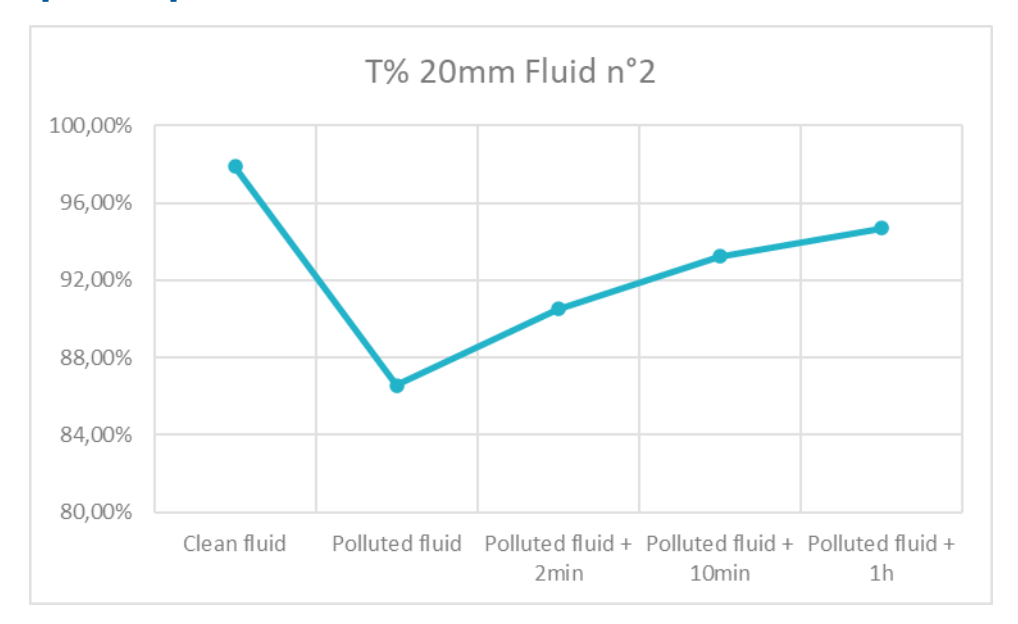


Figure 18: Transmission through a 10mm square quartz cell back and forth, with transmission from the airquartz interface removed. After few minutes, the transmission rises while the pollution settles.



## 4.5 Small signal gain

In this section, all gain are given as single pass "g0L" through the disk assembly. g0L = 0.25 gives a gain of G = 1.65 through the PAMDAM in small signal. The g0L is linked to the total stored energy with the formula :

$$g_0 = \frac{e_{stored}}{\gamma F_s}$$

With the total gain G being linked to g0L in the general case by the Frantz-Nodvik Formula (Frantz, 1 August 1963;):

$$G = \frac{F_s}{F_{in}} \ln \left\{ 1 + \left[ \exp\left(\frac{F_{in}}{F_s}\right) - 1 \right] \exp(g_0 l) \right\}$$

$$F_{out} = GF_{in}$$

- Fin et Fout are in and out beam fluences (in J/cm2)
- F<sub>s</sub> is the saturation fluence of the laser material (in J/cm2)
- g<sub>0</sub>L the small signal gain (no unit)
- L the material thickness (cm)
- e<sub>stored</sub> the stored volumic energy in the laser material (J/cm3)
- γ is the reduction factor of population inversion by 1 photon emission (=1 in 4 level materials like Nd:Glass)

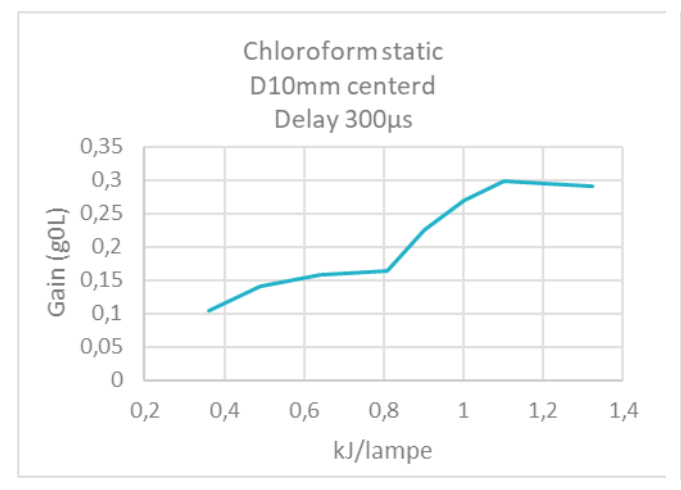
Gain measurement is done in the center of the disks for CHCl4 and Galden HT135 and when it is mentioned over a D160mm beam for AIR and D2O measurement. Gain vs Delay is obtained by delaying the PAMDAM discharge compared to the Q-switch trigger.

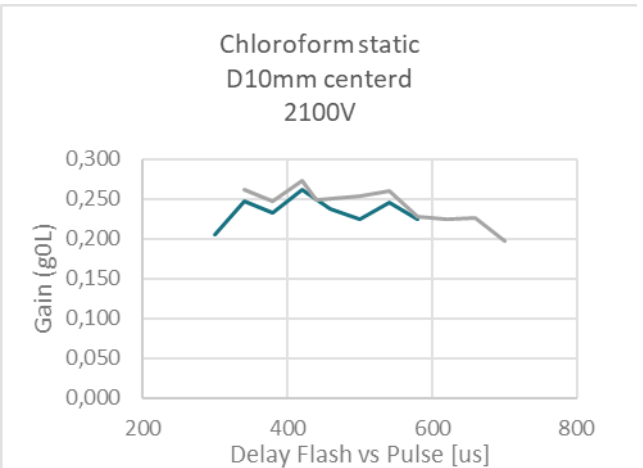
Fluid	Chloroform (CHCl4)	Galden HT 135	Air	D20
g0L small-signal gain	0.3	0.25	0.22	0.305
Stored energy [J]	299	250	219	304

Table 7: Summary of maximal measured gain and derived stored energy for a discharge at 2300V



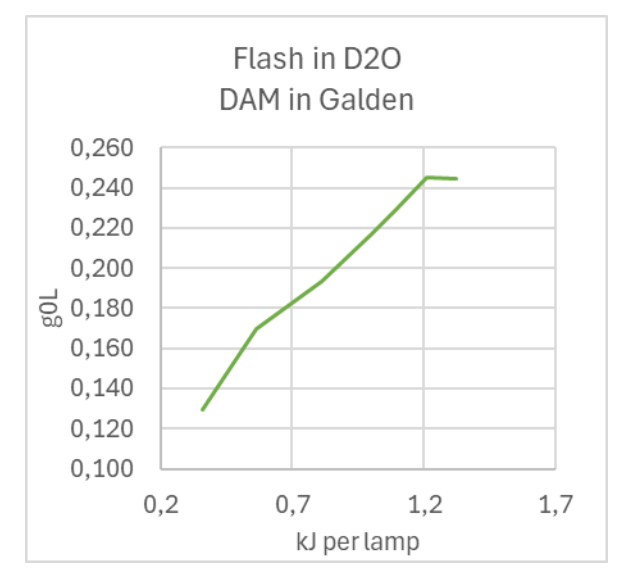
#### 4.5.1 Gain with static Chloroform.





With Chloroform the gain reach 0,3 @2200V, the temporal gain distribution is not very stable, maybe because the fluid start being degraded. As mentioned in the Transmission section, we could only perform this shots before the fluid get black.

### 4.5.2 Small signal gain in Galden HT 135



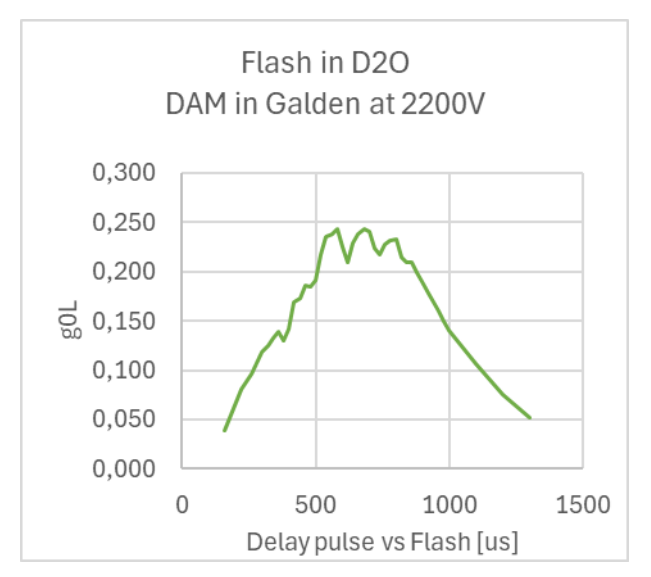


Figure 19: Gain vs energy per lamp with disk assembly in Galden HT 135

Figure 20: Gain vs time for disk assembly in Galden HT 135

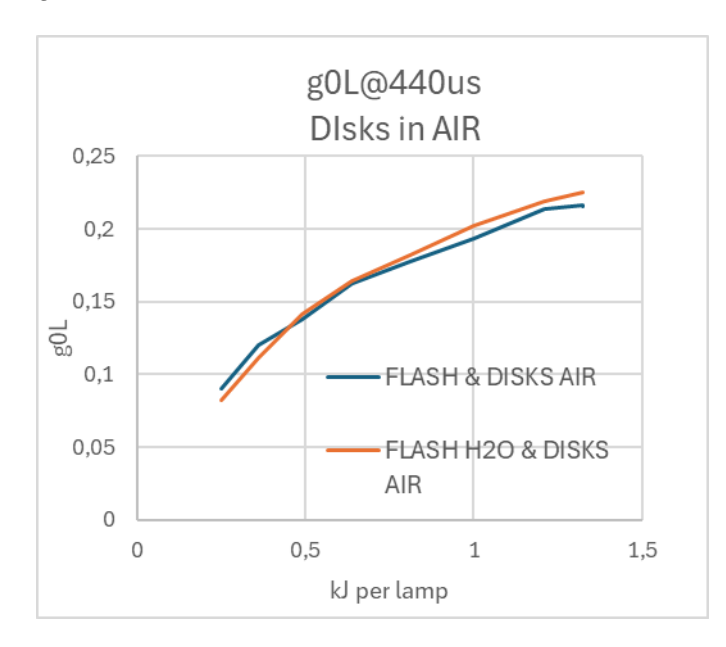
In Galden HT135 the gain reach 0,25 @2200V but stagnate above 2200V. The temporal profile is very unstable with peaks and dips. The stored energy gets spontaneously (i.e. before the probe pulse) depleted before being pumped again by the ongoing discharge then self-depleted, in cycle before the discharge comes to an end. Our explanation is that with a fluid of refractive index 1.28,

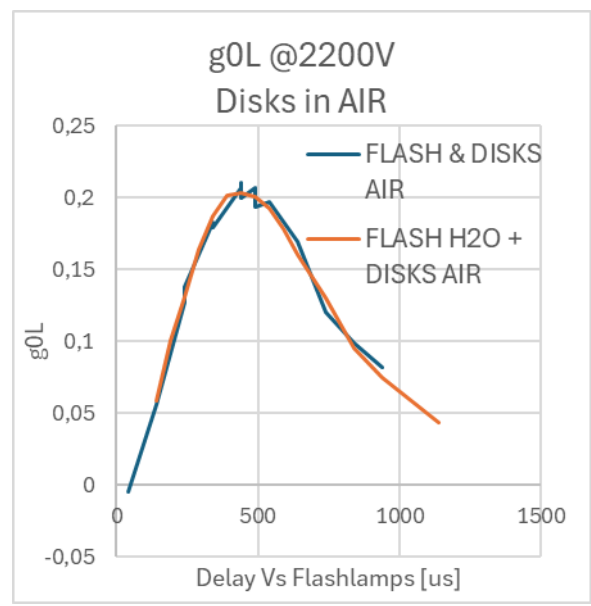


the matching between the disks and the ASE-suppressing cladding is incomplete, leading to transverse ASE depleting the stored energy.

## 4.5.3 Small signal gain in air

We tested two configurations, one with flashlamp and disks in air, the other with Flashlamps in H2O and disks in air. The gain is the same in both configurations, reaching 0.2 @2200V . These results could be interpreted as the coupling of flashlamp is not dependent on surrounding medium, which is surprising considering the refractive index matching the water permits. More likely a strong ASE limits the gain, due to the absence of coupling between the cladding and the disks, and the gain difference with flash in air or in water is lost to ASE.



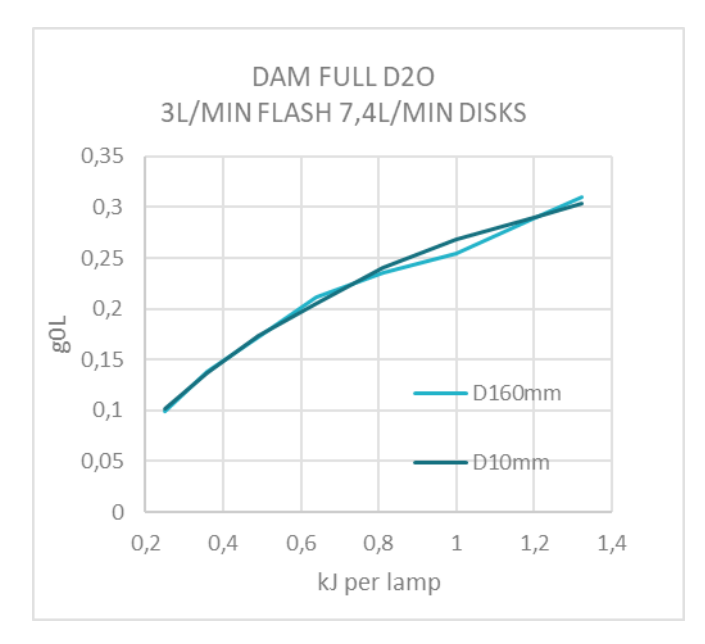


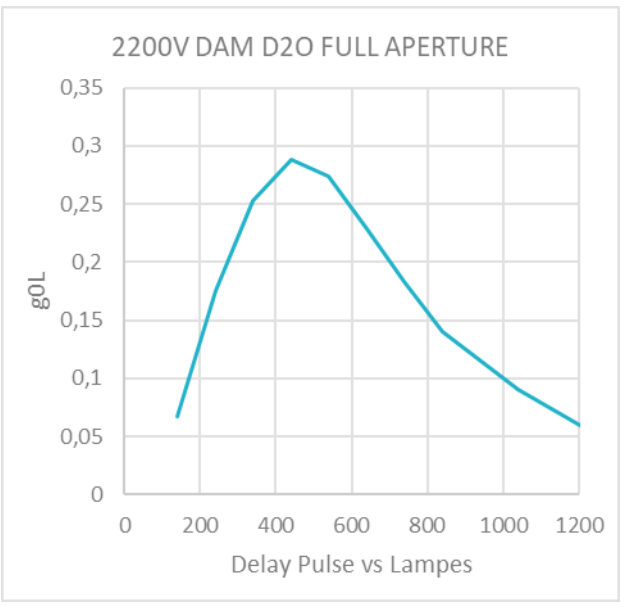


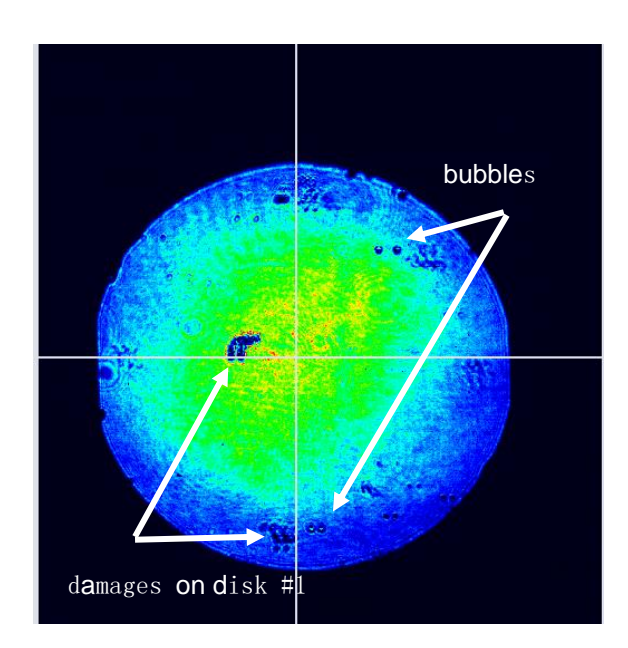
#### 4.5.4 Gain in D2O.

With the PAMDAM filled in deuterium oxyde, both in the flash assembly and the disk assembly, the gain reaches 0.29 with synchronous flashlamps, and 0.305 with one other flashlamps delayed by 100µs. The water is circulating at 3l/min in the flashlamps and 7.4 l/min in the disk assembly. The gain distribution in time is smooth showing no sign of lasing threshold, and significantly less ASE saturation at high voltage.

Tests with a centered Ø10mm beam and full illumination Ø160mm gives the same results.









#### **4.5.5 Gain Map**

We measured Gain spatial distribution by comparing the beam illumination with and without amplification. Care is taken in mitigating and removing the flashlamp background and the camera noise with colored glass Filter RG850 and Interferometric filter at 1053nm (10nm bandwidth). The map shows a very flat gain across D160mm, with noises due to damage on the disks or local variations in the beam distribution.

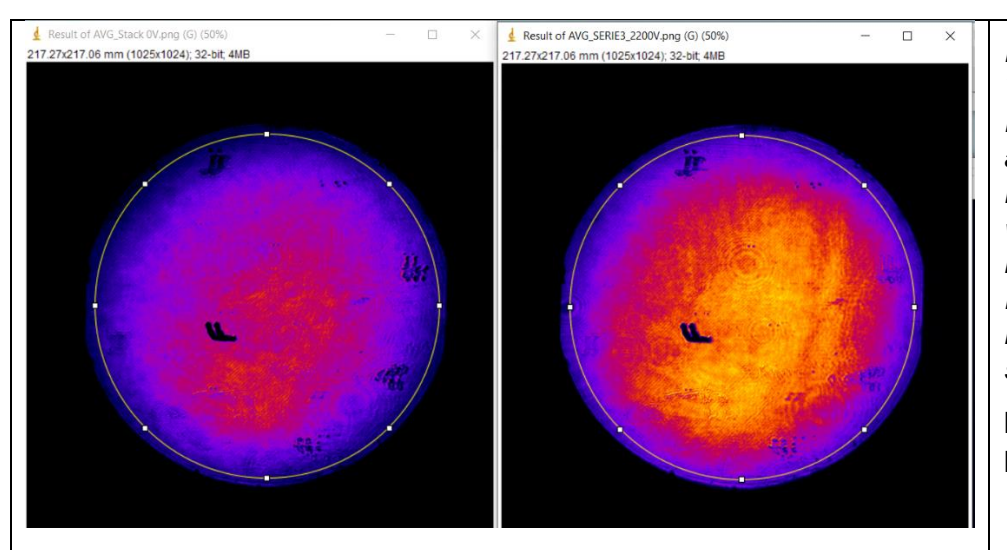


Figure 21: Left:
Transmitted beam at 0V..
Right 2200V
amplification. The yellow
ring is the D160mm disk
where average beam
illumination is measured.
Each image is the mean
if 5 consecutive shots in
similar conditions.

DAM in air, Flash in D2O

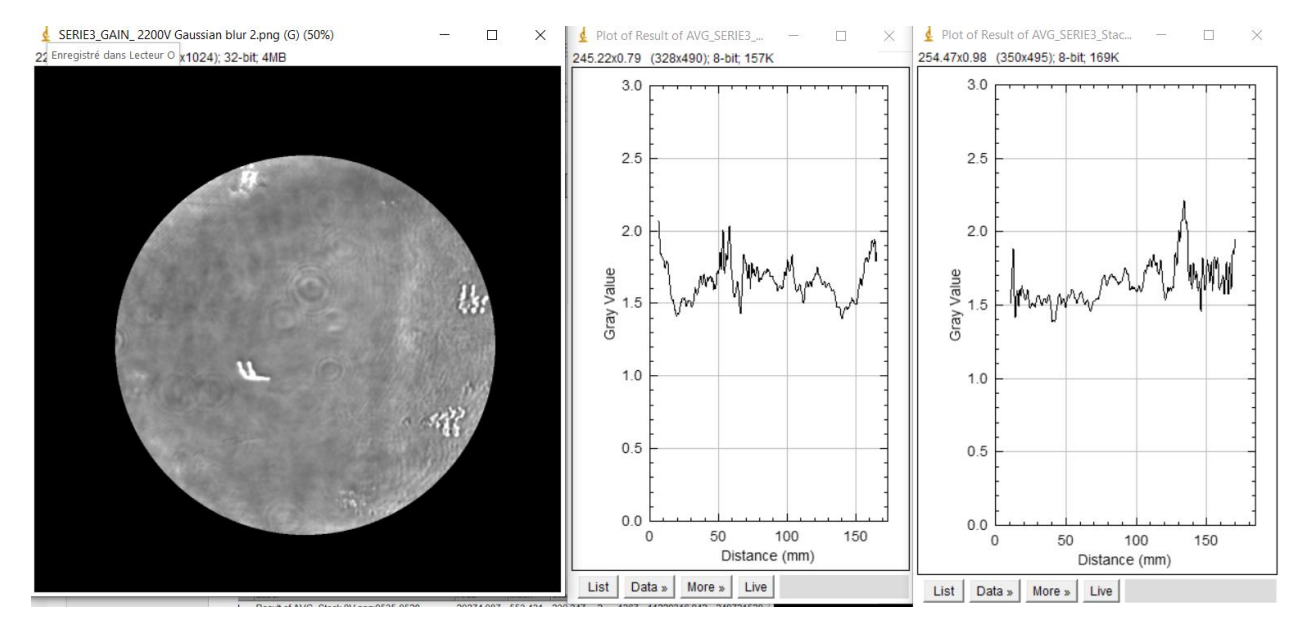


Figure 22 : Gain Map Flash in D2O, Disque in air delay -280s (optimal) Mean g0L sur D160mm = 0,21 (background subtracted)



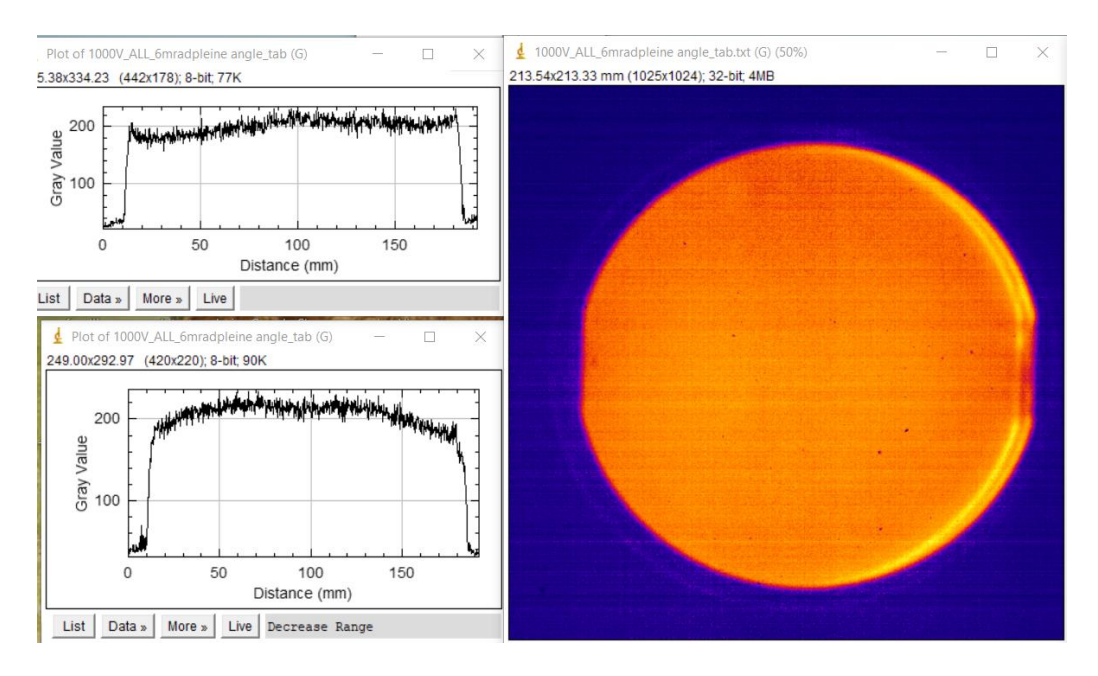


Figure 23: Right : Fluorescence @1053nm @1000V (color scale normalized). Top Left : Vertical Lineout. Bot Left : Horizontal Lineout.

### 4.6 Fluorescence

## 4.6.1 Experimental apparatus:

Fluorescence light is incoherent and emitted with a wide angle. Imaging such light source can result in vignetting if the f-number of the imaging system is too low. The camera is set with 1ms exposition time with interferometric filter 1053nm with 10nm BW.

A solid aperture in an intermediate plane limits the solid angle of collection to 6mrad -increasing the effective f-number-, equivalent to a collection angle on the DAM of 0.3mrad. It results in a vignetting effect of only 0.6mm at the edge of the disk.



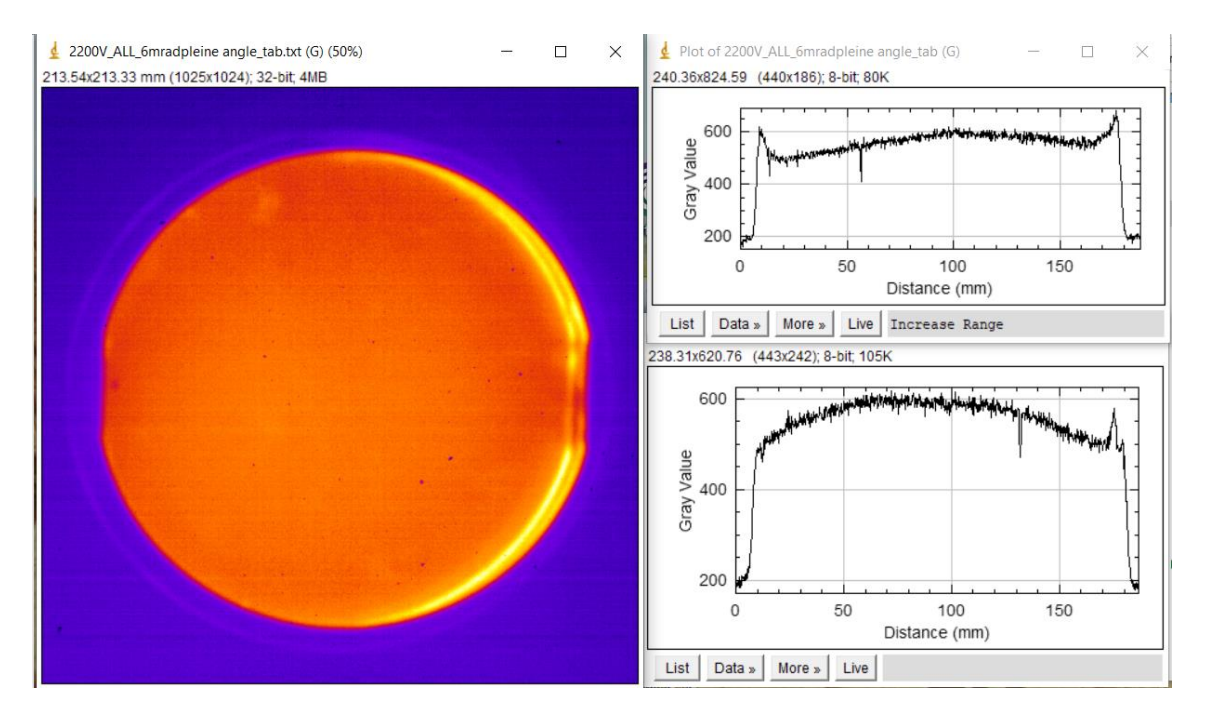


Figure 24 : Left : Fluorescence @1053nm @2200V (color scale normalized). Top right : Vertical Lineout. Bot right : Horizontal Lineout.

Fluorescence maps show the same distribution at 1000V and 2200V with no spatially dependent parasitic self-lasing that may occur at high voltages.

# 4.7 Birefringence

# 4.7.1 Birefringence Apparatus

The incoming beam is P-polarized with two Brewster angle polarizer resulting in a better than 1:5000 polarization ratio.

A polarizing cube with an extinction ratio of 1000:1 is installed in the collimated beam before the camera. The ratio of S to P average illumination is computed with the help of calibrated ODs. The ratio of the maximum of illumination in both pictures is named "Max depolarization" while the ratio of the mean illumination in Ø160mm is "Mean depolarization."

The birefringence of the amplified beam is computed with removal of the fluorescence background in pol S (the one with the fewer attenuation)



## 4.7.2 Birefringence without disk cooling

Configuration	Flow rate in Flashlamps	Voltage	Mean Depolarization	Max Depolarization
NO SLAB/NO DICHRO EXT	0 l/min	0V	0.16%	0.25%
NO SLAB/NO DICHRO EXT	4.5 l/min	0V	0.14%	0.22%
NO SLAB + DICH EXT	0 l/min	0V	0.17%	0.24%
SLAB 1 only	0 l/min	0V	0.18%	0.31%
Complete DAM in AIR	0 l/min	0V	0.30%	0.60%
Complete DAM in AIR	4.5 l/min	0V	0.31%	0.79%
Complete DAM in AIR	4.5 l/min	2200V	0.24%	0.39%
+5min at 2 shot/min	4.5 l/min	2200V	0.22%	0.83%
+10min at 2 shot/min	4.5 l/min	2200V	0.20%	0.54%

Table of birefringence for the disks in air data above shows that :

The depolarization is kept low with and without flashlamp pumping, showing the low stress applied to the optics. The pressure in the Flashlamp assembly does not rise the birefringence. Half of the static depolarization comes from the window between the lamp and the optical assembly. The other half comes from the laser disks. None comes from the front external dichroic mirror. The depolarization distribution evolves with lamp pumping but stabilize after 10min.



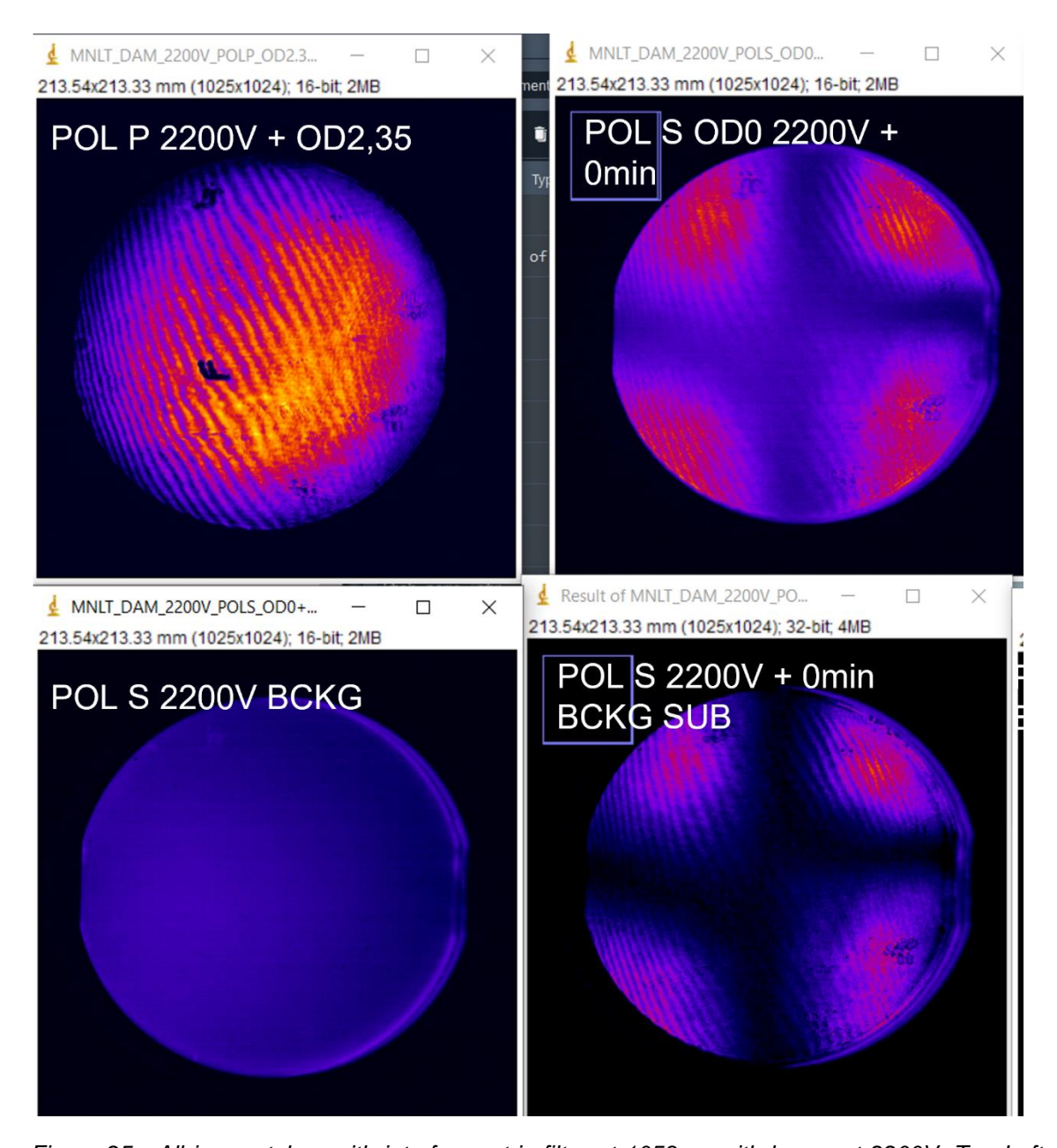


Figure 25: All image taken with interferometric filter at 1053nm with lamps at 2200V. Top Left: Amplified beam in pol P + OD 2.35. Top right: amplified beam in pol S, no ODs. Bot left: No beam, background in pol S from flashlamps. Bot right. Amplified beam in Pol S with subtracted background.



#### 4.8 Wavefront Distortion

#### 4.8.1 Experimental Apparatus

The PAMDAM plan is imaged on a 4-waves shearing interferometer from Phasics (SID4 HR, 9.98 x 8.64 mm², 416 x 360 phase pixels). Aberrations from the optical test bench alone are measured thanks to a reference flat Ag Mirror installed in place of the PAMDAM. All measures are presented in reference from this FLAT surface if not mentioned otherwise. Two steps are implemented to improve the wavefront stability:

- The Q-switched cavity source is pinholed to amplify only a TEM00 mode. M<sup>2</sup> goes from 4~5 to 1.1 at the source exit.
- A cover limits the air movement around the optical test bench.

It results in a stable source wavefront. Removing the Astigmatism and Spherical aberration from the optical test bench, the Strehl ratio is 0.99 and very stable.

All Aberration are given PV (Peak to Valley) in  $\lambda$  (1053nm) over a Ø160mm analysis pupil. The Strehl ratio (SR) is the ratio between the peak intensity at a focal point for the real aberrated system versus a perfect aberration-free optical system. It is a merit parameter that can be linked to the wavefront phase root mean-square by the following formula:

$$SR \sim e^{-\sigma^2}$$

The wavefront distortion can be separated into four main contributions:

- The passive contribution (optics bulk and surface quality, mechanical constraints on the optics)
- The pressure contribution (from the cooling fluid flow)
- The dynamic aberration (from the flashlamp shockwave)
- The thermal aberration (rising over time from thermal accumulation in the disks and optics)

#### 4.8.2 Results for a passive DAM (no water flow)

Without any water flow or flash pumping, a combination of astigmatism ( $\sim$ 1  $\lambda$  PV) and defocus ( $\sim$ 0.4  $\lambda$  PV) and Spherical Aberration (AS  $\sim$ 0.16  $\lambda$  PV) is applied to the beam. Even by removing such low order aberrations (such aberrations could be easily removed by a deformable mirror), the Strehl ratio is degraded to 0.8 showing that high order aberrations sum up as well.

By removing each optical component one by one we could track back the origin of both low order and high order aberrations.



The external dichroic mirror does not change the wavefront properties. By removing the laser disks one by one, the high order aberration disappears and comes back to same level as with the FLAT reference mirror. High order aberrations are measured through the **Residual Strehl ratio** – Strehl ratio when Focus, Astigmatism and Spherical aberrations are removed.

Without disks, only the same low order aberration remains but with a much better residual Strehl ratio going **from 0.8 to 0.96**. Therefore the low order aberrations are caused by the mount of the window, or the internal dichroic mirror.

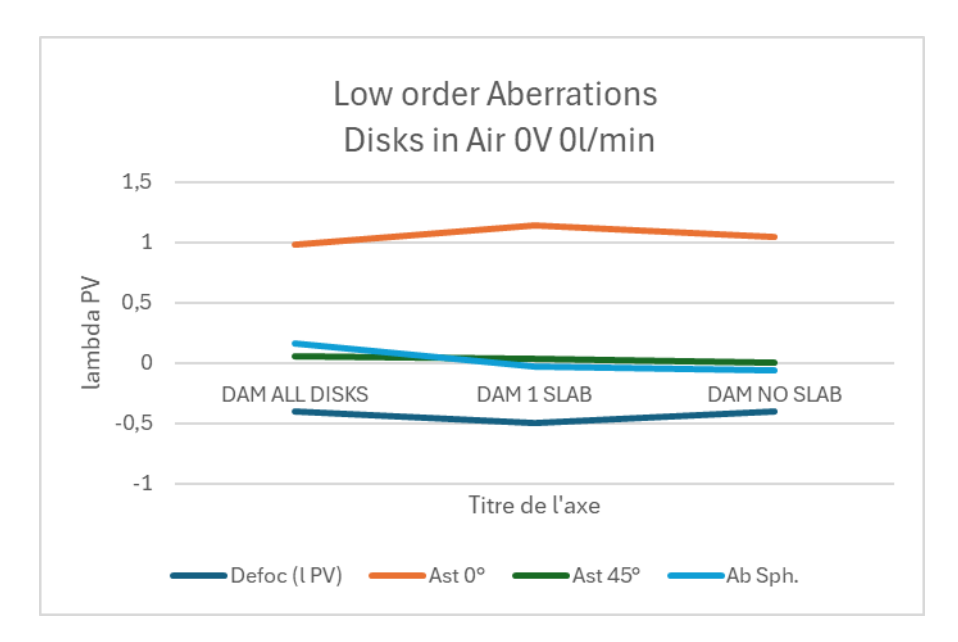


Figure 26: Low order aberrations in different conditions, without flashlamp, with static water in the flashlamp.

Disks do not contribute to these aberrations.



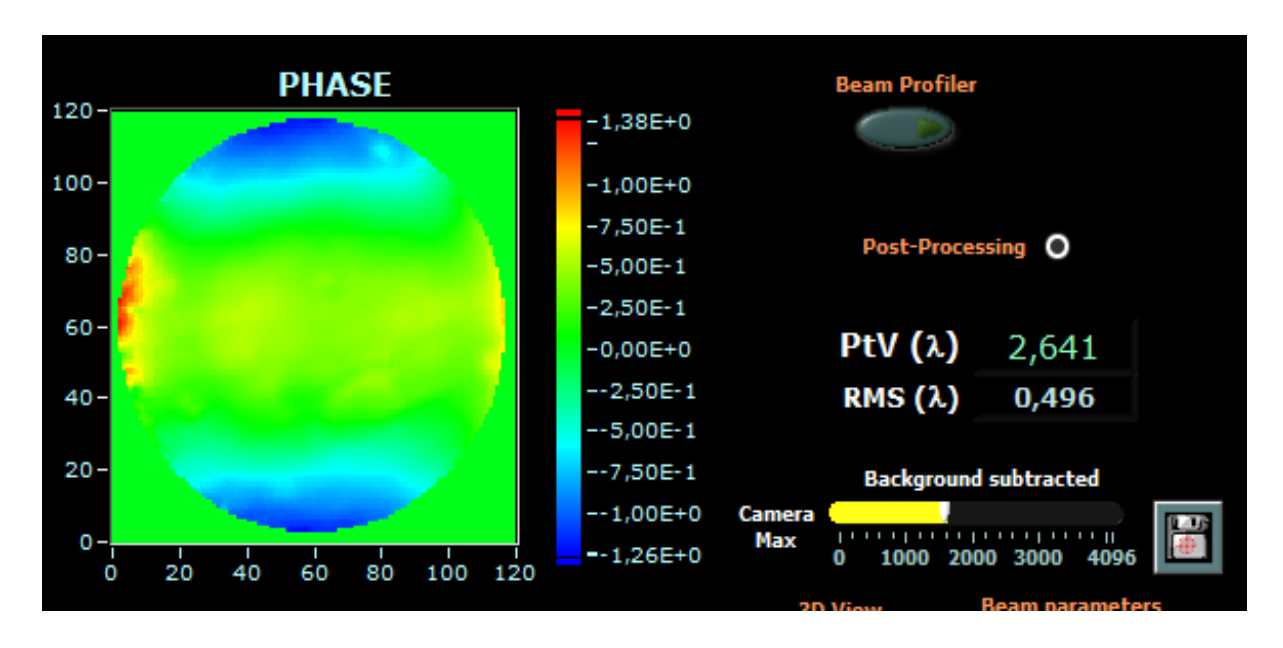


Figure 27: Passive Deformation applied by the DAM at 0V 0l/min with all disks and dichroic mirrors. REF FLAT

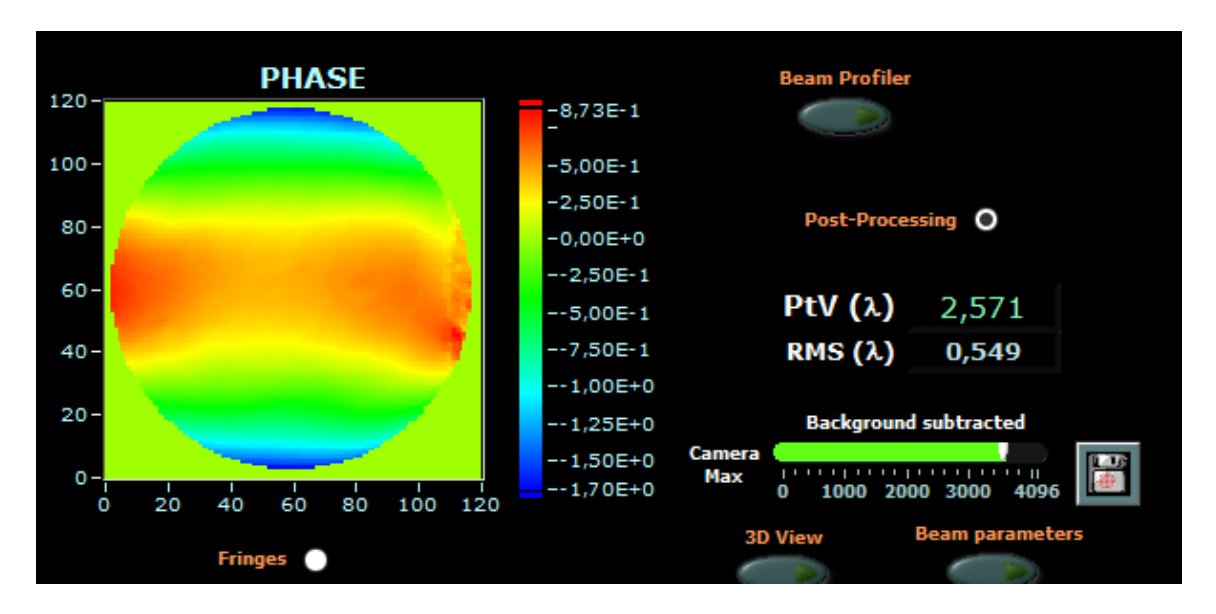


Figure 28: Passive deformation applied by the DAM at 0V 0l/min without disks. REF FLAT



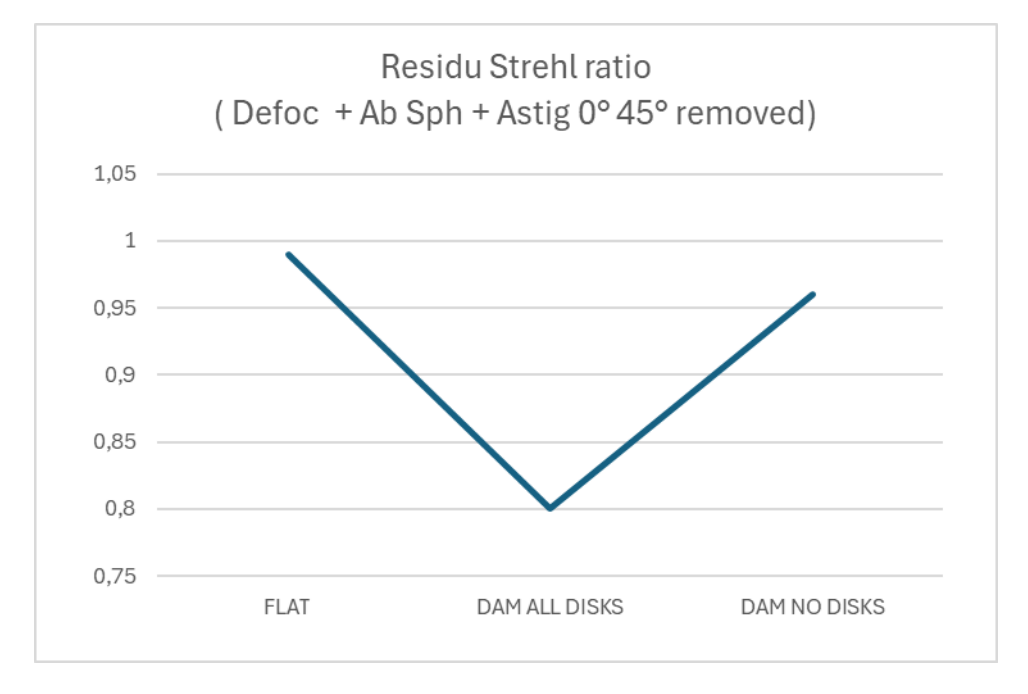


Figure 29: Residual Strehl ratio in different configuration with disks in Air. DAM 0V 0l/min is the full optical assembly in static condition, with no water flowing in the flash assembly. Disks are degrading the Strehl ratio.

## 4.8.3 Water pressure effect

### 4.8.3.1 With Air in the optical assembly

To separate the contribution of various optical elements to the aberration we study in this section the wavefront without laser disks, with air in the optical assembly.

By flowing water in the flashlamp assembly, the window and dichroic mirror are constrained, and severe astigmatism aberration occurs. Such deformation must be compensated for by equal pressure in the optical assembly on the other side of the window.

The window bulge creates a water lens, leading to a converging beam in the horizontal dimension and leading to strong positive astigmatism at 0° (+6.5  $\lambda$ PV) + positive focus (+1.5  $\lambda$ PV). This effect is observed by removing the laser disks to be sure to observe only the window + water + internal dichroic contribution.



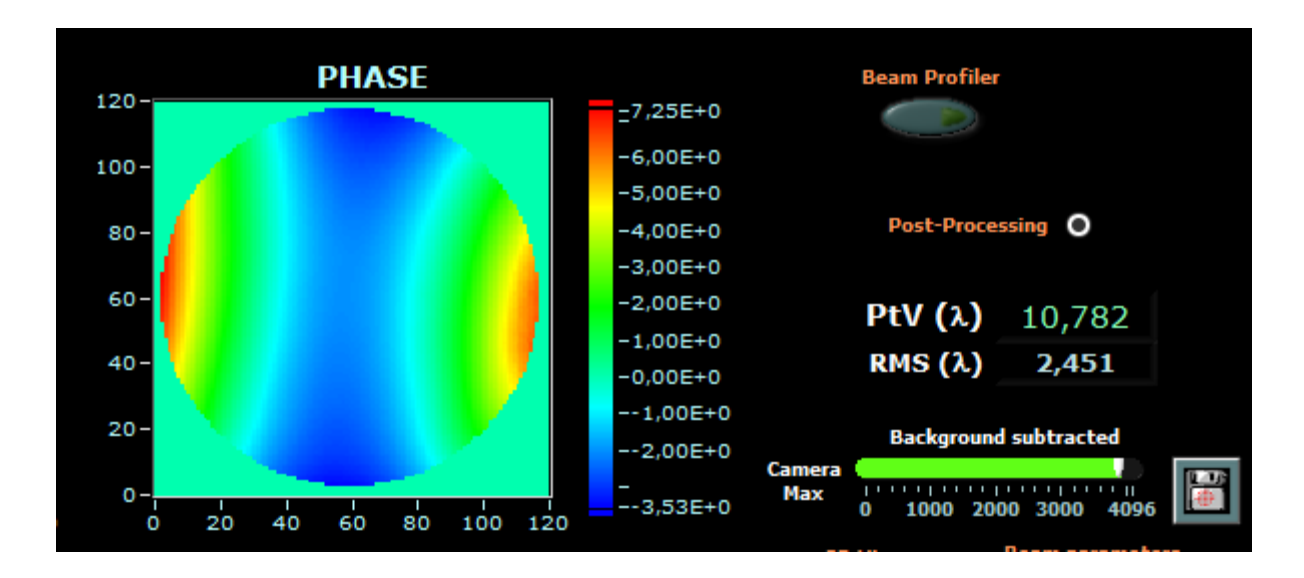
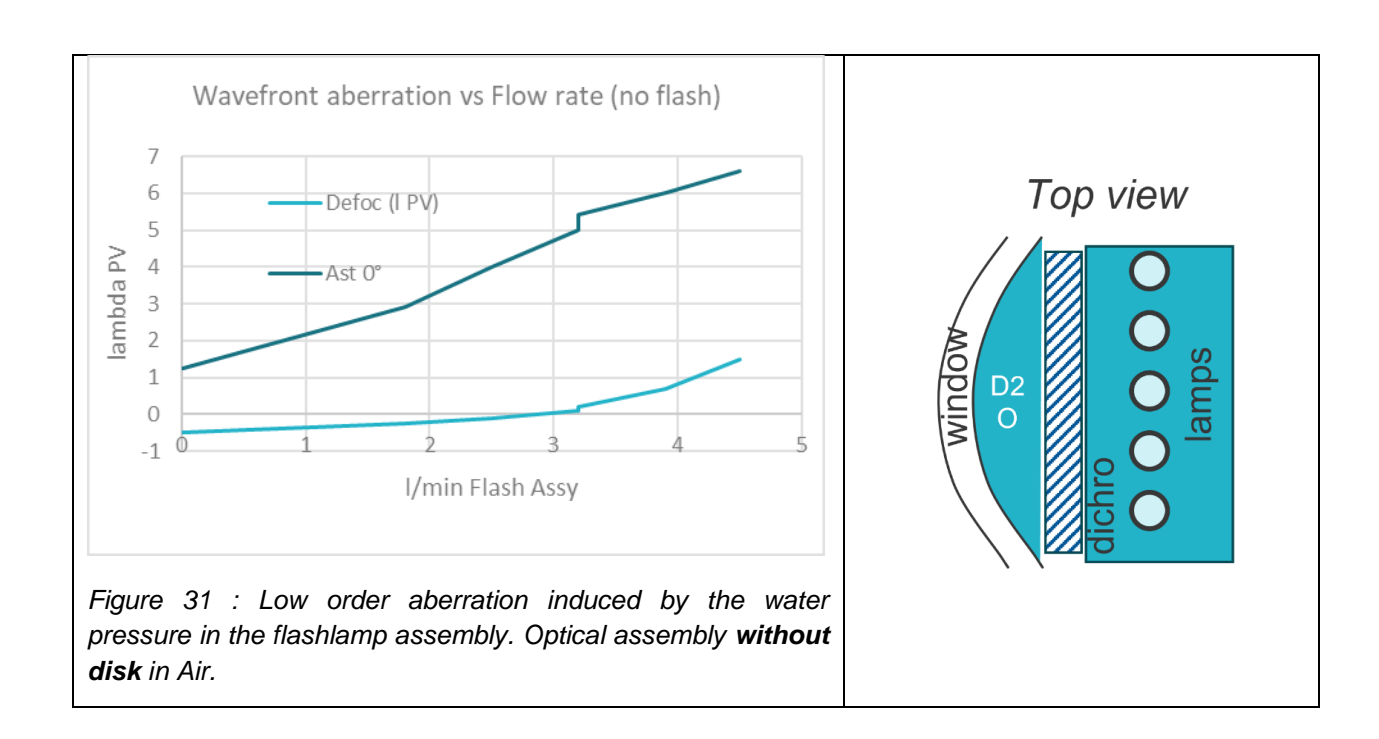


Figure 30 : Wavefront deformation with DAM without disks, in air. 0V Flashlamp assembly on 4.5l/min - 0.5 bar. REF FLAT



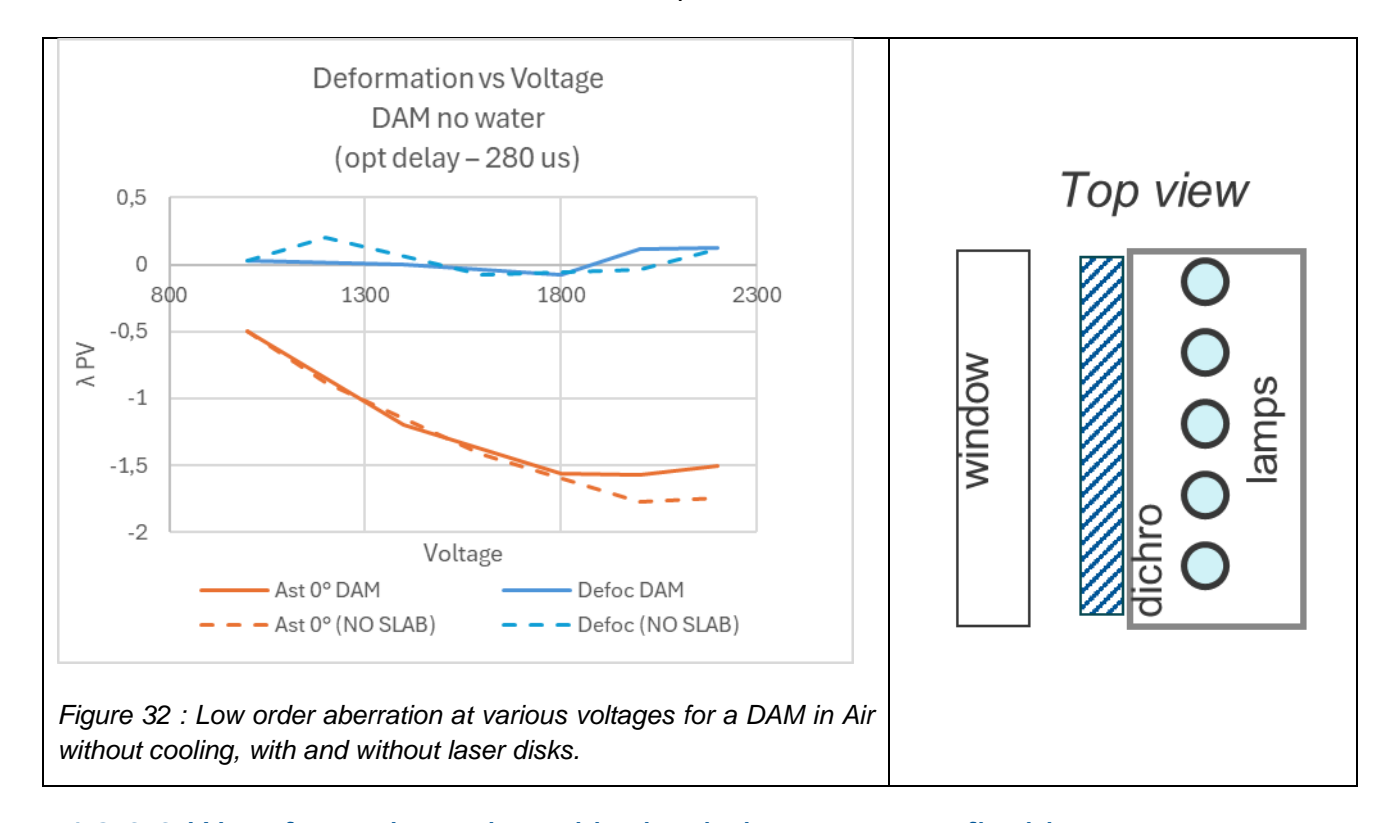
As the water bulges create a water lens, it hides the shockwave effect on the optics (dichroic mirrors and window).

## 4.8.3.2 Air in both disks and flashlamp assembly

It was possible to shoot the flashlamp without cooling at 1 shot/4min, with both flashlamp and disk assembly in air, without damage. We can observe the contribution of the shock to the mechanical mount adding mostly astigmatism as the voltage rises. The disks have no immediate contribution,



as they are not constrained by the discharge. Nonetheless, a thermal lens occurs after dozens of shots, described in the "Thermal wavefront" chapter.



## 4.8.3.3 Wavefront aberration with circulating water, no flashlamps

When the PAMDAM is complete with water flowing in both assemblies, the strong aberrations disappear, because the window bulges in the same medium. The following table shows the limited effect of the water pressure on the PAMDAM aberrations when water is circulating. No dependency on the water flow is noticeable. The wavefront aberration is below 2  $\lambda$ PV with low order aberration below 0.7  $\lambda$ PV and the high order contribution from the disk degrading the residual Strehl ratio to 0.85.



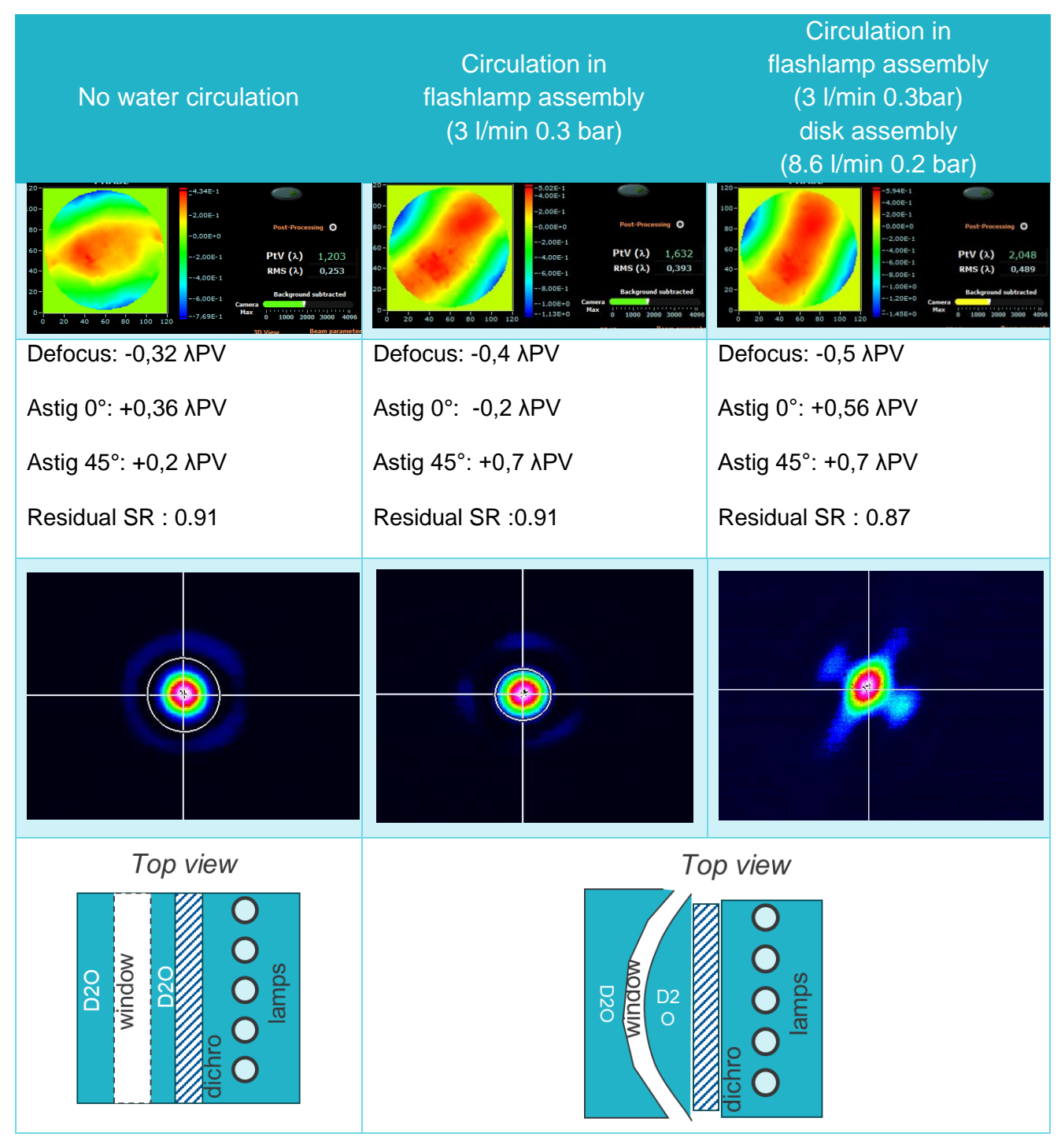


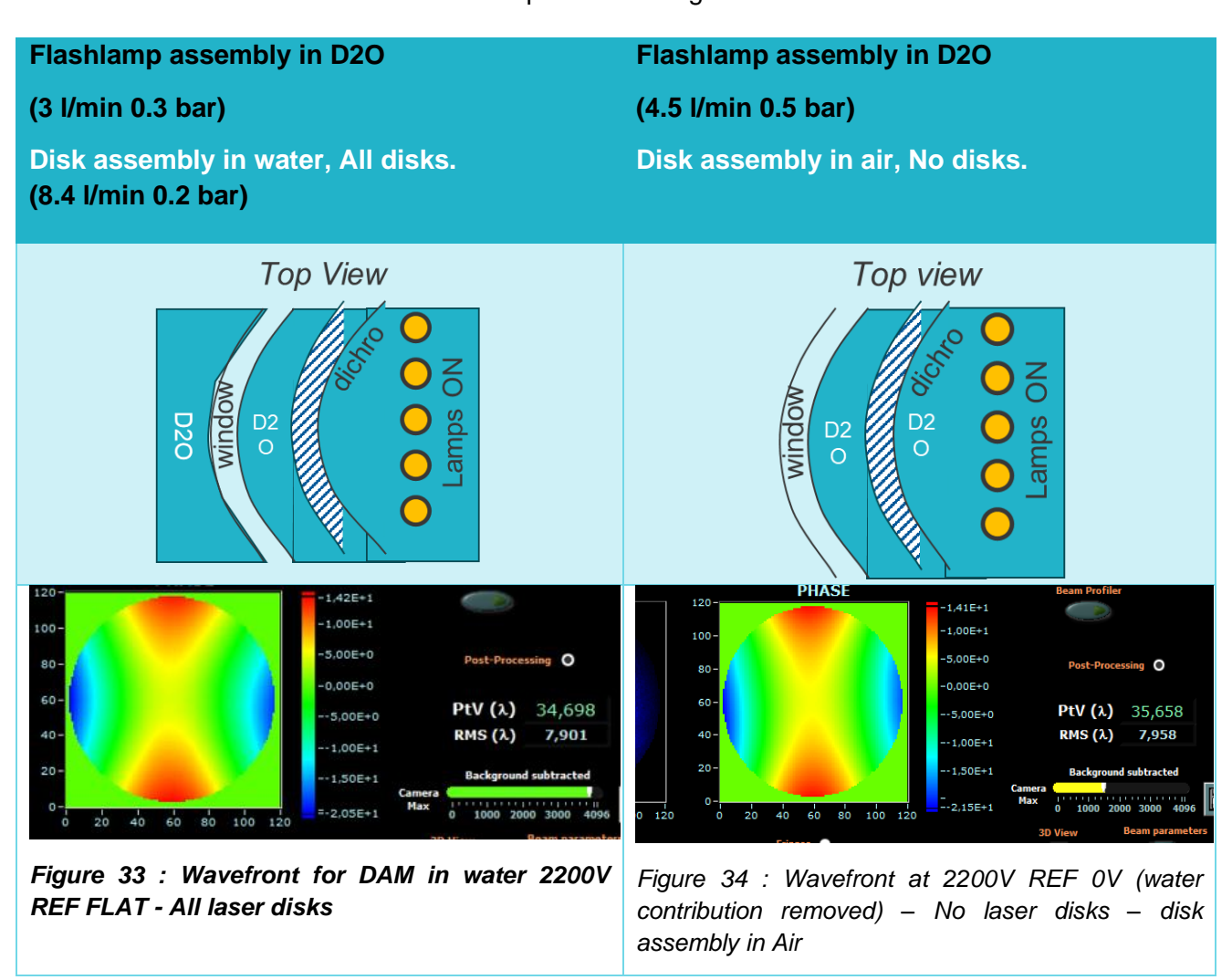
Table 8: Wavefront deformation in various conditions of fluid circulation. Bottom left: far field at a focus of a f470mm lens of the D160mm probe beam. Diameter of the first extinction = 270  $\mu$ m. Bottom mid: scheme of the window bulge when flashlamp assembly is on 0.3 bar of pressure. Bottom right: far field at a focus of a f470mm lens when flashlamp assembly is on 0.3 bar of pressure.



## 4.8.4 Effect of flashlamp discharge - No laser disks

During lamp discharge, a shockwave is sent through the water and deform the optics, curving the internal dichroic mirror. It leads to a strong negative astigmatism  $0^{\circ}$  (-18  $\lambda$ PV) and defocus (-5  $\lambda$ PV). Such deformation is monitored both with the PAMDAM full of circulating water vs with no disk, with the optical assembly in air.

The dynamic of this deformation is monitored through time by varying the delay between the probing pulse and the flash discharge. The curve shows the contribution of the discharge alone – with the static deformation from the water pressure being removed -



Flashlamp assembly in water

(3 I/min 0.3 bar)

Disk assembly in D2O, All disks. (8.4 l/min 0.2 bar)

Flashlamp assembly in water

(4.5 l/min 0.5 bar)

Disk assembly in air, No disks.



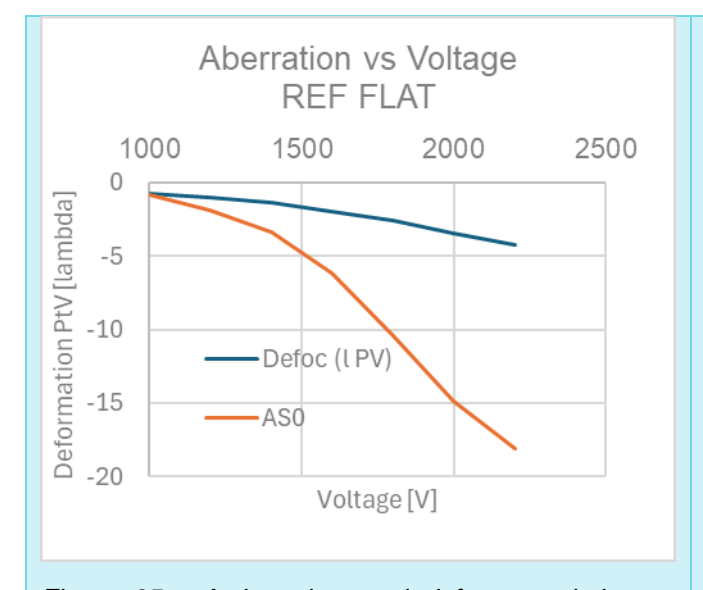


Figure 35 : Astigmatism and defocus variation vs flash voltage at optimal delay for amplification. REF FLAT, All laser disks

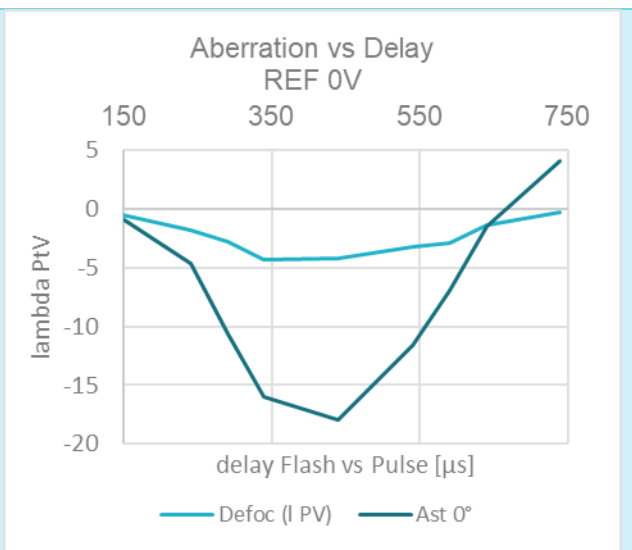


Figure 36 :Temporal variation astigmatism 0° and focus during the discharge, REF 0V (passive contribution are removed)

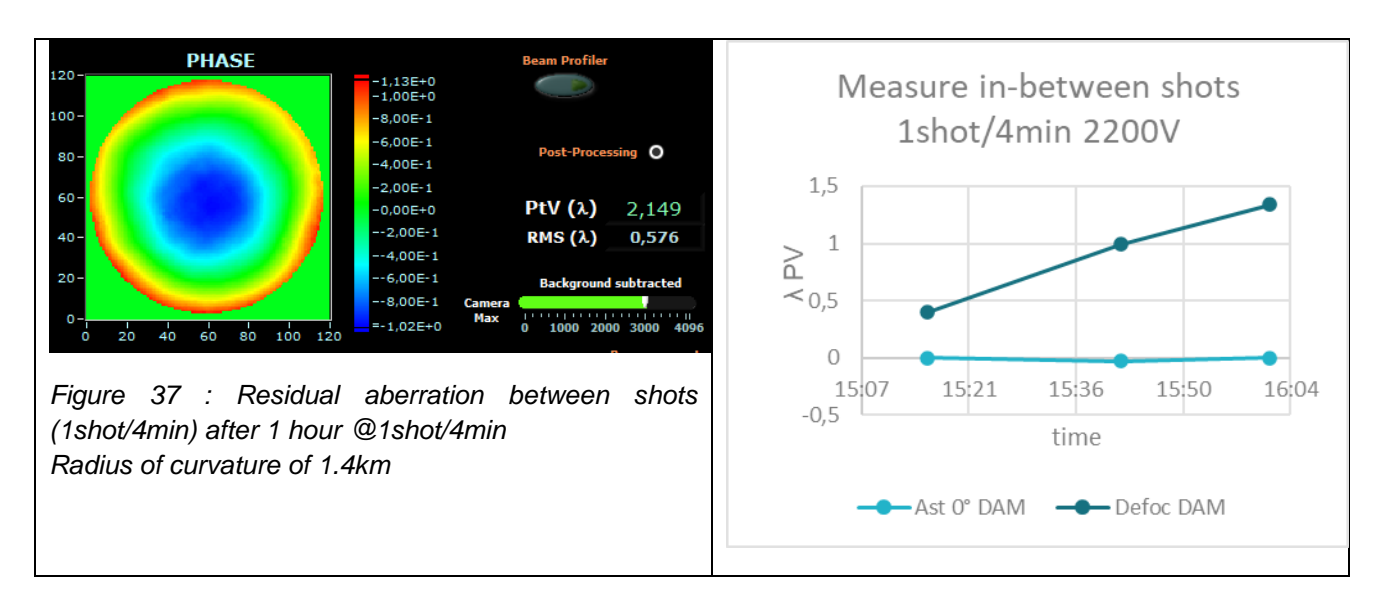


### 4.8.5 Thermal contribution to the wavefront

The wavefront at the nominal delay for the amplification is heavily distorted by astigmatism, but the thermal aberration accumulation can be monitored by probing the PAMDAM between lamps discharges. Two tests have been performed, one with running water at 2shot/min, and the second without cooling, in air at 1shot/4min.

#### 4.8.5.1 DAM with flash and laser disks without water.

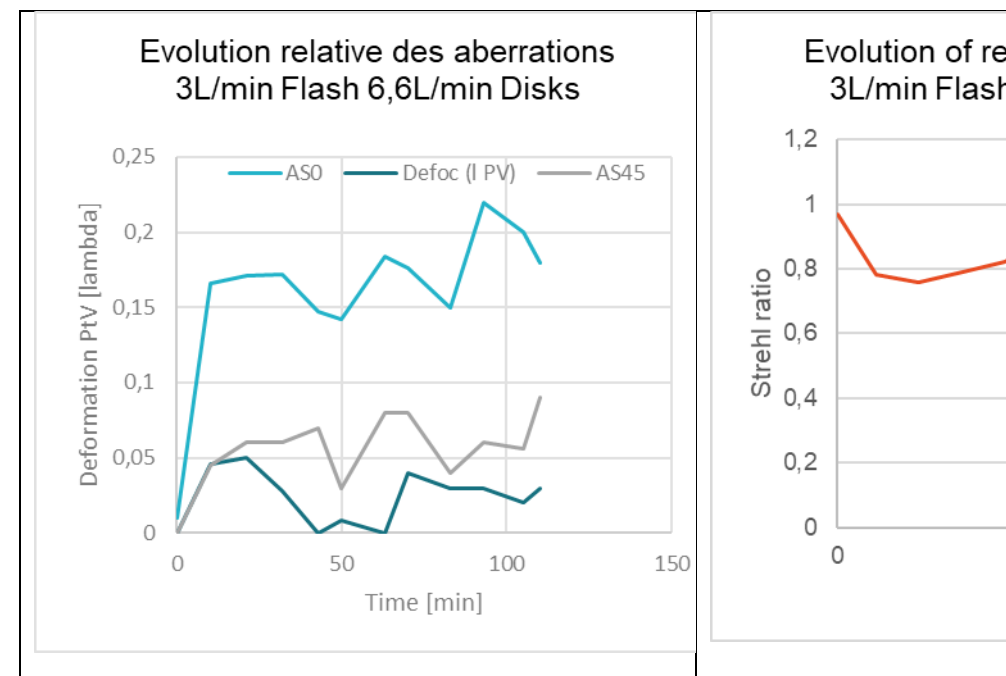
PAMDAM is set without water to remove excessive dynamic astigmatism, at 1shot/4min. No added defocus is visible on the first shot. Astigmatism up to  $-1.8\lambda PV$  is added by the discharge but is the same with or without the laser disks. A residual contribution in defocus is added by thermal loading of the disks shot after shots and should be eliminated with adequate cooling, reaching 1.4km after 1 h. No other aberrations are observed.

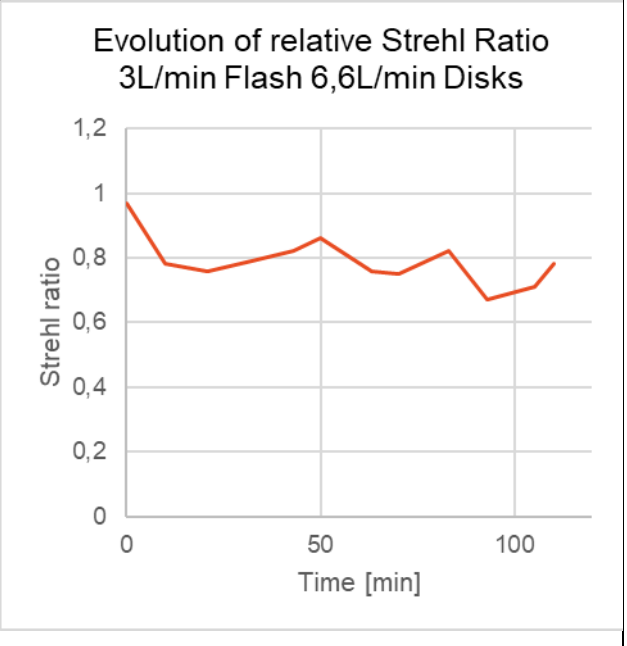


## 4.8.5.2 DAM with cooling water.

The following graph monitors the evolution of aberrations between shots at 2shot/min with disks being cooled in water at 6.4 l/min. A phase reference is taken at 0min, and the left figure shows the evolution of low order aberration relatively to this reference. On the right side, the figure shows the evolution of relative Strehl ratio, 1 being the SR at 0 min. Aberrations are low ( $<0.2 \ \lambda PV$ ) in amplitude and settle after 10min. Strehl ratio is decreased due to the astigmatism building up but settle at 0.8 after 10min, while the test lasted 2h.







### 4.8.6 Wavefront measurement conclusion

#### 4.8.6.1 Low order aberration

While the low order aberration is very low in static configuration, both for the back optics (internal dichroic, flashlamp assembly window) and the optical bloc (laser disks, external dichroic), the water pressure and the lamp shockwave, induce a strong deformation of the back optics, mostly in the form of defocus and astigmatism.

Laser disks show very little contribution to low order aberrations under the lamp shockwave. A low ( $<0.2~\lambda PV$ ) thermal astigmatism builds up over 10min when the PAMDAM is water-cooled and shoot at 2shot/min. It is likely that this aberration is not coming from the disks, as without cooling it was shown that disks alone only build up defocus (1.4km focal lens after 1h).

## 4.8.6.2 High order aberration

The Residual Strehl ratio is the Strehl ratio computed by SID4 software when low order aberrations are removed (Defocus, Astig 0° & 45°, Spherical Aberration). It is a measurement of the contribution of all other high order aberrations to the focal spot quality. The Strehl is typically equal to this formula:

$$Spprox e^{-\sigma^2}$$

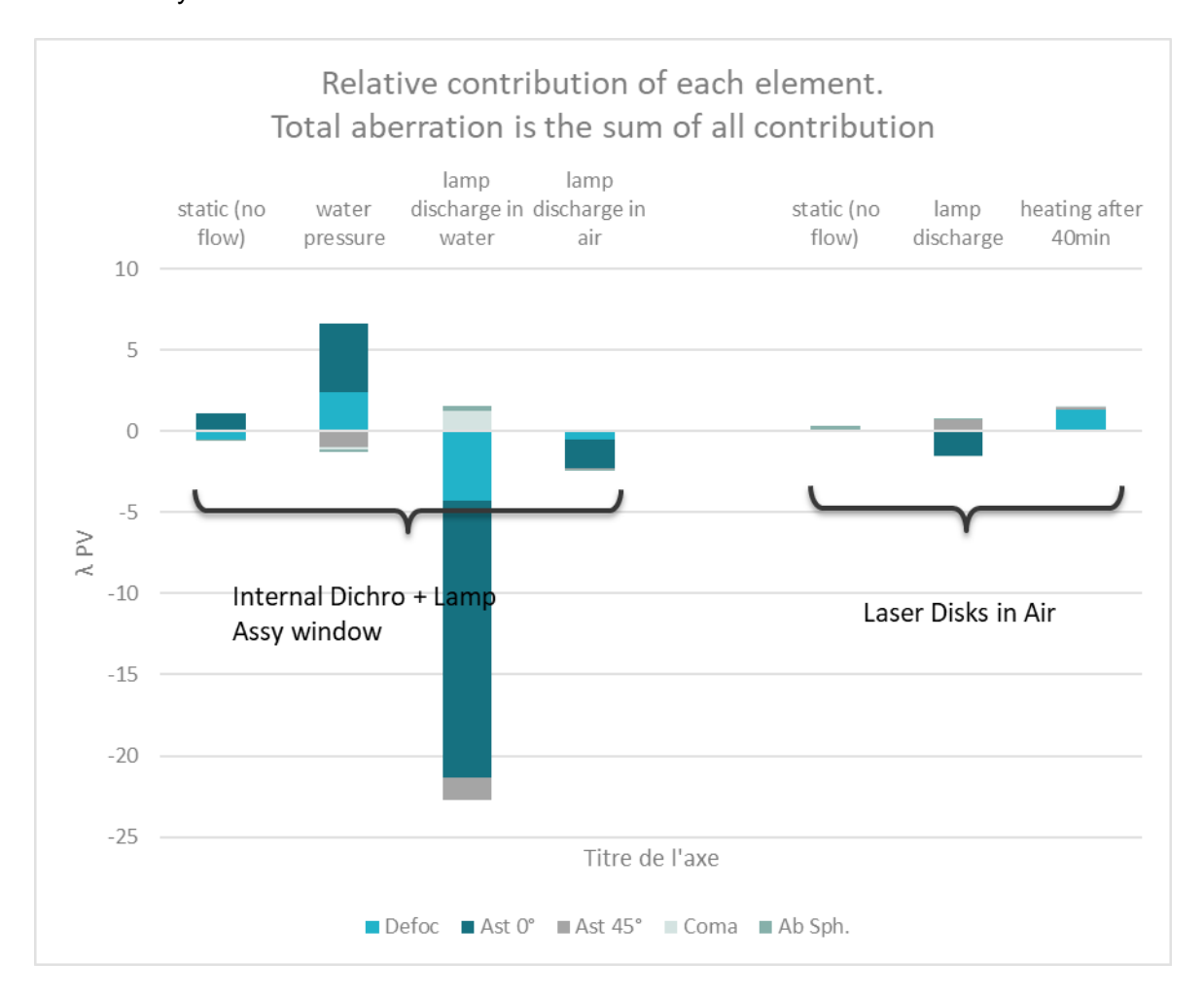


where  $\sigma$  is the root mean-square deviation over of the wavefront phase.

Both dichroic mirrors and the window have no high order contribution, with a residual Strehl ratio of 0.96. Laser disks on the other side contribute to the degradation of the Strehl ratio to 0.8 -0.7 in static condition.

The strong shockwave of the flashlamp decreases the Residual Strehl ratio to 0.05 if it propagates in water. In Air no additional contribution to the high order aberrations is induced by the discharge nor the heating, and the Residual Strehl ratio is kept ~0.8.

A residual Strehl ratio of 0.8 per PAMDAM is a strong degradation because it may be non-corrected by a deformable mirror.





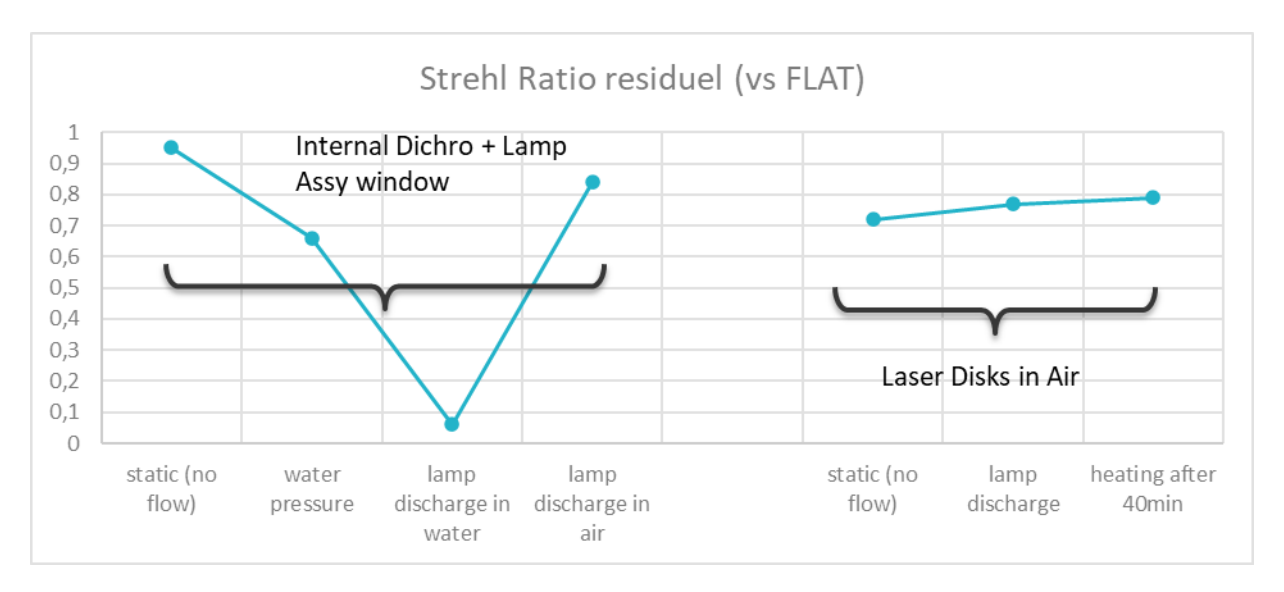


Figure 38 :Residual Strehl ratio (Strehl Ratio while removing defocus, astigmatism and spherical aberration) from different contributions, all compared with a FLAT reference.

### 4.8.6.3 Design Take-out

In the current configuration, where the window is an interface between two medium of different refractive indexes (water vs air) the water pressure and the lamp shockwave induce aberrations above what would be an acceptable value for a deformable mirror.

On the other hand, the laser disks make little contribution to low order aberration and limited heat deformation. But their bulk and surface quality degrade the Strehl ratio with aberration not correctible by a deformable mirror. Extra care must be taken in the handling and protection of laser disks from humidity. Water in the air slowly etch the disks bulk and lead to more laser diffusion.

## 4.8.7 Fringes from the water flow

Heating of the laser disk could also be visible in the water flow running in thin channel between disks. On previous high rep rate PAMDAM D100mm in YAG, vertical fringes appear, damaging the laser profile in propagation. Water refractive-index variation to temperature is 2,6x10<sup>-3</sup>/K. Local transverse velocity variation of the cooling fluid can affect the temperature, and results in aberrations with a comb-like structure, resulting in fringes after few meters.

Here specific attention is given to flow homogeneity. The absence of fringes is observed in virtual propagation by moving the near field camera downward according to the classical optic laws. If a Keplerian (2 positive lenses f1 > f2) telescope have a demagnification of 1/G = f1/f2 then moving the camera by  $\Delta z$  downstream image a plan located  $\Delta z \times G^2$  downstream from the previous imaged plan.



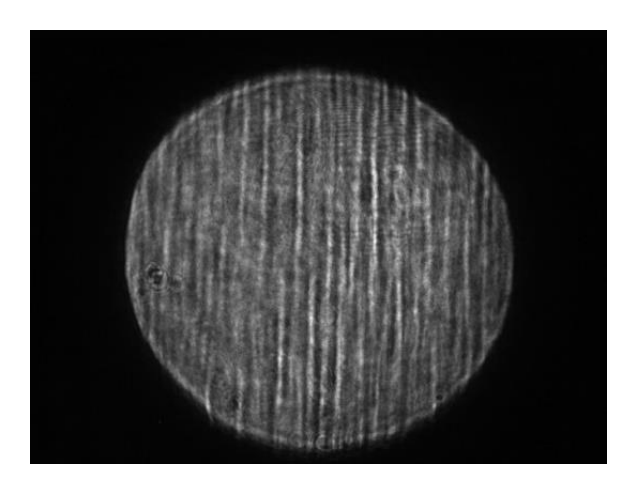


Figure 39: Example of flow fringes due to inhomogeneity of temperature and flow velocity in the D100mm YAG PAMDAM (500W to dissipate):

> No visible franges from the water flow

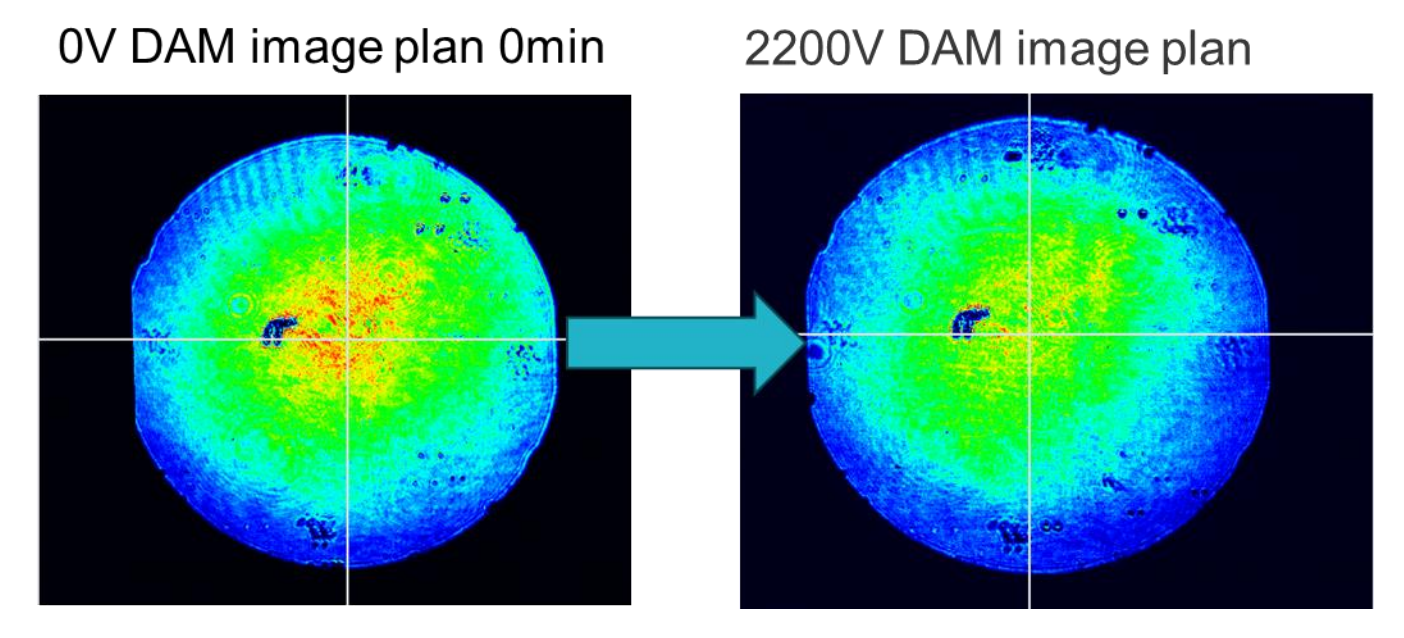
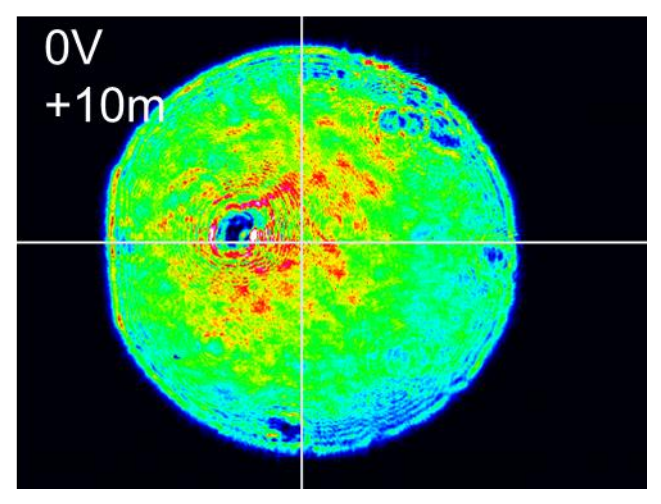


Figure 40: Near Field image of the beam at 0V or at 2200V after 30min at 2 shot/min in the image plan of the PAMDAM. DAM in circulating water. Color level is normalized for each image.





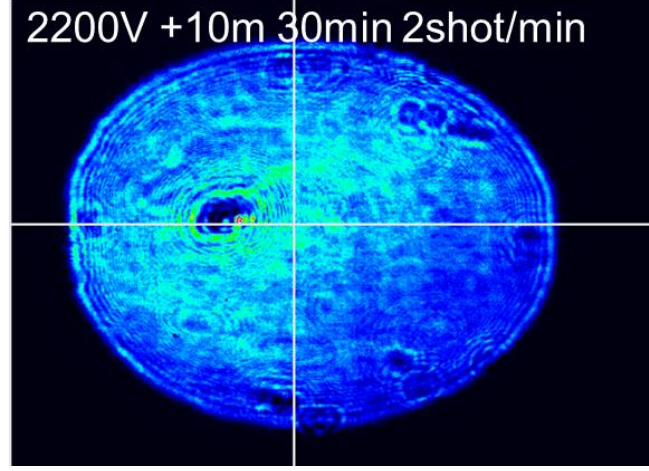


Figure 41: Near field after 10m of propagation. 0V DAM in circulating water. Dark spots are damages on the first disk due to water degradation and burned chloroform.

Figure 42: Near field after 10m of propagation. 60thshot at 2shot/min 2200V. DAM in circulating water. Astigmatism from the discharge is clearly visible, as explained in the wavefront section, but no fringes are visible.

# 4.9 Pointing Stability

Pointing stability is observed at the focal point of a lens of focal +470mm, after demagnification of the beam by a x1/20 Keplerian telescope. Stability is acquired with a Beamage 3 camera. The large variation of astigmatism during each shot, highlighted in the previous section, prevents us from acquiring shot to shot focal position. We saw that removing the water from the flash assembly limit the dynamic astigmatism to  $-1.5\lambda PV$ , low enough that the focal spot can be track from shot to shot. We performed the acquisition in such condition at low rep rate (1shot/4min without cooling).

Our source and diagnostic bench have a static pointing stability of 12.3 $\mu$ rad RMS (after the demagnification x1/20, therefore ~0.6 $\mu$ rad RMS for the Ø160mm beam). But the discharges at 1000V lead to large drift of the beam angular direction as shown in the following figure. At 2200V the pointing stability is too unstable to be meaningful, varying of **more than 2mrad** over 2h30.

A severe problem in the dichroic mount needs to be addressed. It is probable that the strong shock from the flash lamp moves the dichroic mirror in its mount and the spring-loaded "finger" that hold it in place do not reposition the mirror in the same place after each shot.



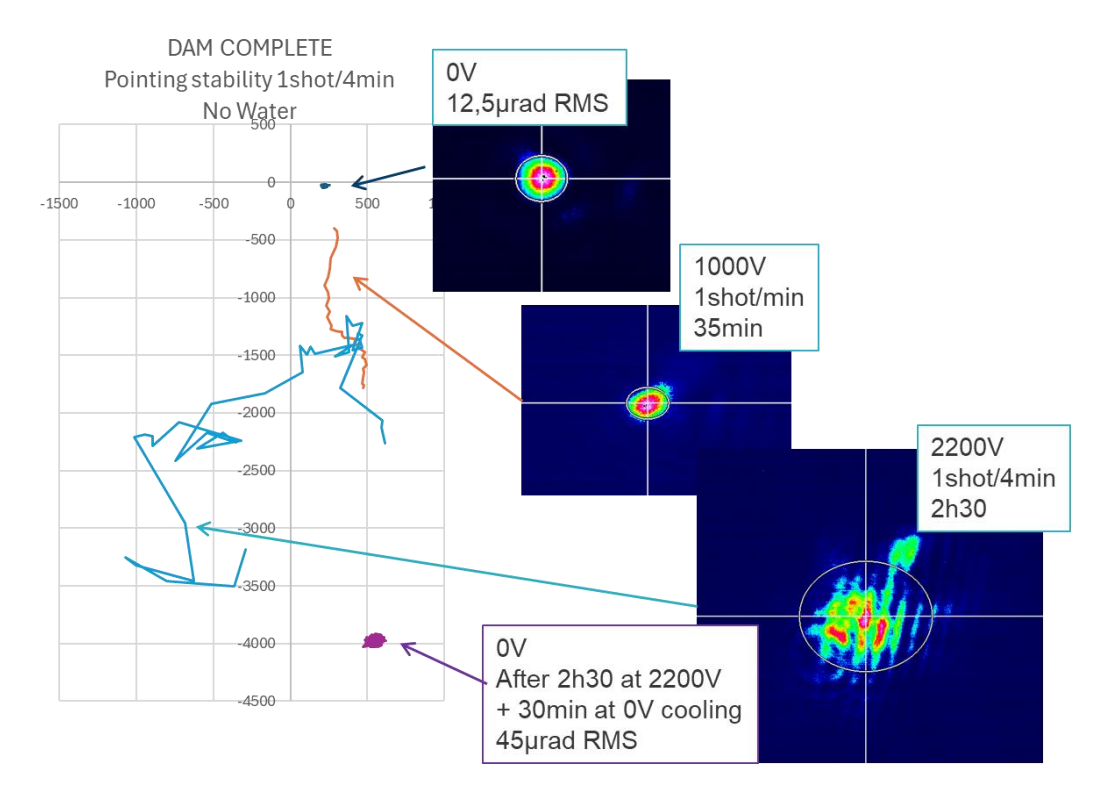


Figure 43: focal spot position (in µm) on the Beamage 3 camera for different condition. dark blue, static stability without discharge. Orange: drift at 1000V 1shot/min. Light blue: focal position at 2200V 1shot/4min. Purple: static stability without flash after 30min of cooling.



# 5. Conclusion

This present work of the PAMDAM Ø200mm explored novel ideas of great interest for the high energy laser community and paved the way for a new amplifier compatible with kJ laser system at 1 shot/min.

The experience of Amplitude in the domain of large Pseudo-active mirror amplifier enabled the project to focus on new development while the ground technological components were already robust:

- Assembly of more than one thousand pieces for the PAMDAM without mechanical design errors.
- No leaks despite Optics/Metal interfaces, discharge shockwaves, and a new flashlamp assembly. No corrosion after 1 year.
- Power supply, capacitors banks, and flashlamps fired for 10k+ shots without missed shots or instable trigger.
- Procurement and test of challenging large optics performed in time.

Novel ideas were assessed for the first time in a liquid-cooled amplifier.

- Innovant cooling fluid test: Chloroform and Toluene were tried for the first time in laser environment. Galden HT135 was evaluated for the first time with close coupling to the flashlamp and we discovered degradation never mentioned in literature.
- The geometry for improved coupling proved to be beneficial for the stored energy. Coupling simulation prevision matched the results despite limited literature on lamp cross absorption/reemission.
- Highlight of the critical effect of ASE mitigation on the stored energy. The stored energy is consistently higher when the coupling between the disks and the ASE-suppressing cladding is better.
- Demonstration of a stored energy (300J) /small-signal gain (0,3) unmatched for such liquidcooled active mirror Nd:Glass amplifier.
- Thanks to the flow shaping before the channel, the flow homogeneity was good enough to avoid any fringes at high rep rate. (2shot/min)

Nonetheless, three difficulties require more development to achieve an efficient Amplifier.

1. Use of water as a cooling fluid can only be temporary, as degradation of the disks leads to



more diffusion, and prevents the use of adequate coating to improve transmission.

- 2. Without an index matching liquid, the coupling between the cladding and the disks cannot be achieved with the current configuration. Adhesion of the cladding to the disk should suppress the building of parasitic oscillation and ASE whatever the cooling fluid choice.
- 3. The flashlamp shockwaves in water leads to a large (>  $30\lambda$  PV) deformation of the dichroic mirror, and to its pointing instability. We think the proximity of the dichroic mirror to the flashlamps, and its mounting structure, are to blame.

# 5.1 Project continuity

In the framework of the THRILL Project, the PAMDAM prototype should be sent to the LULI for implementation into a beam recombination experiment in July 2025. But the current status of the PAMDAM does not meet stability requirements of the LULI to perform their experiments:

- The use of water to cool the disks degrades them and surface damages are already visible.
- The pointing stability is erratic at high voltage, requiring a re-work of the dichroic mirror mount.
- The large lamp shockwave drives an aberration of more than 30λPV at each shot, making the fine recombination of such beam impossible.

In order to fix these issues, 3 main research axis for future projects are envisioned:

- I. Does an air-cooled PAMDAM at 1shot/min achieve correct heat extraction without adding wavefront deformations?
- II. Which adhesion process is sufficient for suppressing parasitic oscillation, and can it sustain the harsh condition of flashlamp irradiation?
- III. How to improve the optics holding to resist the flash shockwave?



# 6. Bibliography

Andy Bayramian, J. A. G. B. R. C. B. C. R. C. A. E. Y. F. B. F. R. K. J. M. W. M. K. S. C. S. S. J. T. S. T. & Barty, C., 2008. High-average-power femto-petawatt laser pumped by the Mercury laser facility. *Journal. Opt. Soc. Am. B*, Volume 25, pp. B57-B61.

Batani D, C. A. C. F. e. a., 2023. Future for inertial-fusion energy in Europe: a roadmap.. *High Power Laser Science and Engineering.*, p. 11:e83. .

Condamine, F. P. J. N. K. D. T. P. G. A. F. G. .. &. W. S., 2022. Commissioning results from the high-repetition rate nanosecond-kilojoule laser beamline at the extreme light infrastructure. *Plasma Physics and Controlled Fusion*, Volume 65(1), p. 015004.

D. Brown, J. K. a. J. A., 1981. Active-mirror amplifiers: Progress and prospects. *IEEE Journal of Quantum Electronics*, 17(9), pp. 1755-1765.

Frantz, L. M. N. J. S., 1 August 1963;. Theory of Pulse Propagation in a Laser Amplifier. *J. Appl. Phys.*, p. 34 (8): 2346–2349.

Garrec, B. L., 2022. *Bilan de fonctionnement du laser CNE400 - APO-WP0-BLG-20220112-Bilan-CNE400-B*, s.l.: LASYEX S.R.O. pour LULI-APOLLON.

Hernandez, J. A. S.-R. N. T. R. B. S. D. A. B. G. M. O., Branly, S. & Mollica, F., 2024. The high power laser facility at beamline ID24-ED at the ESRF. *High Pressure Research*, Volume 44(3), p. 372–399.

Kelly, J. H., D. C. B. J. A. A. a. K. T., 1981. Dynamic pumping model for amplifier performance predictions. *APPLIED OPTICS*, p. 1596.

Linford, G. J., December 1994. Time-resolved xenon flash-lamp opacity measurements. *Applied Optics*, p. 8333.

Mason, P. D. M. E. K. P. J. B. T. H. M. .. &. C. J., 2017. Kilowatt average power 100 J-level diode pumped solid state laser. *Optica*, Volume 4(4), , pp. 438-439.

Pierre-Marie Dalbies, S. C. E. B. N. B. J. G. M. a. J. N., Nov 2023. Analysis of mid-spatial frequency wavefront distortions from a liquid cooled flash-lamp pumped Nd:phosphate laser amplifier. *High Power Laser Science and Engineering*.

Roland S. Nagymihály, F. F. B. B. J. B. V. P. L. L. M. R.-S. O. R. S. C. F. M. S. B. P.-M. P. Á. B. K. V. G. S. & Kalashnikov, M., 2023. The petawatt laser of ELI ALPS: reaching the 700 TW level at 10 Hz repetition rate. *Opt. Express,* Volume 31, pp. 44160-44176.